ENVIRONMENTAL FACTORS AFFECTING PLANKTONIC FORAMINIFERA ABUNDANCE AND DISTRIBUTION IN THE NORTHEAST GULF OF MEXICO

A Thesis

by

SHARATH REDDY RAVULA

Submitted to the Office of Graduate Studies of
Texas A&M University
in partial fulfillment of the requirements for the degree of

MASTER OF SCIENCE

May 2004

Major Subject: Oceanography

ENVIRONMENTAL FACTORS AFFECTING PLANKTONIC FORAMINIFERA ABUNDANCE AND DISTRIBUTION IN THE NORTHEAST GULF OF MEXICO

A Thesis

by

SHARATH REDDY RAVULA

Submitted to Texas A&M University
in partial fulfillment of the requirements
for the degree of

MASTER OF SCIENCE

Approved as to style and content by:

Niall Slowey (Chair of Committee)	John Wormuth (Member)
Mitch Malone (Member)	Wilford Gardner (Head of Department)

May 2004

Major Subject: Oceanography

ABSTRACT

Environmental Factors Affecting Planktonic Foraminifera

Abundance and Distribution in the Northeast Gulf of Mexico.

(May 2004)

Sharath Reddy Ravula, B.S.M.E., Columbia University

Chair of Advisory Committee: Dr. Niall Slowey

The shell composition of planktonic foraminifera used in many paleo-reconstructions assumes they are accurately representing conditions at the surface/mixed layer. However, planktonic foraminifera are known to inhabit a depth range that extends below the mixed layer. In the present study, foraminifera were collected at discrete depth intervals using a Multiple Opening and Closing Net Environmental Sensing System (MOCNESS) in either cyclonic or anticyclonic eddies that had contrasting environmental conditions. The foraminifera abundances and distributions were compared to the water depth, temperature, density, and chlorophyll profiles. Nine species were found consistently among all the tows and composed at least 96% of the species found, though a shift in the species abundances and depths occurred between eddies. Species occurred where physical factors were compatible with conditions and feeding opportunities they were adapted to. Three species pink and white *Globigerinoides ruber* and *Globigerinoides sacculifer* thrived best when a steep density gradient resulted in a shallower mixed-layer that restricted them under more intense light and allowed them to better exploit their algae symbionts. *Globigerina bulloides* was found outside its sub-polar habitat because the waters of the cyclones were cool enough (less than 26°C) at the same depths that sufficient chlorophyll was available. Two

species *Orbulina universa,* and *Globorotalia menardii* were consistently absent in the mixed layer, but tracked deeper chlorophyll concentrations. Three other species were found inconsistently among the tows: *Hastigerina pelagica, Globigerinella siphonifera,* and *Globigerinella calida. H. pelagica* probably follows chlorophyll concentrations. *G. siphonifera,* and *G. calida* have a preference for deeper waters within the photic zone. The drastic doubling to tripling of the foraminifera abundances in cyclones biases downcore reconstructions of sea surface temperature towards cooler conditions. Also, the shift in species composition between the two eddies indicates that in environments where eddies, upwellings, or rings exist may bias the downcore composition of each species towards cooler conditions. *G. sacculifer* was found to live primarily in the mixed layer and at least 75% of its downcore individuals are expected to represent conditions there. Researchers should consider the described species distributions to better understand the water column conditions they are reconstructing.

DEDICATION

I am blessed in that I can do what I enjoy the most with the support of my loving family and friends without whom this work would not have been possible. Even those of you who have left me here have continued to send me your love and support. After you read this dedication, call and remind me that I owe you dinner, a cool beverage, and a few stories.

ACKNOWLEDGMENTS

I would like to thank my friends, family, and everyone I worked with while I conducted my research. I would like to especially thank the people below for their specific contributions to my thesis.

Dr. Niall Slowey, Dr. John Wormuth, Dr. Mitch Malone provided me intellectual guidance, office, laboratory space, equipment, comments, suggestions, and patience. Dr. Doug Biggs provided me with the complete GulfCet II hydrographic data and the appropriate calibration data. Dr. George Jackson helped me with the gradient plots (Figures 13-21). Sandy Drews provided me with a foil for my pranks and wit, and helped me navigate through university paperwork. Commander Ed Shaar (retired) supported me when my previous advisor left and provided me with three semesters of support.

I would also like to thank the other graduate students in the department. Dan Bean helped me with the myriad hardware, software, and other gripes. Debora Berti helped me get started in Illustrator and in Java programming. Darin Case got me through the Departmental inventory, safely. Amy and John Bratcher let me live with them and let me occasionally win. Brian Brookshire helped me with statistics, and the SPSS plots (Figure 9&10). Rob Cady helped me survive my microscope work and taught me how to get myself in shape. Susie Escoria helped me survive my first advisor. Simone Francis checked that my mathematical explanations made sense. I need to thank Dr. Patrick Ressler for the template of the GulfCet map with the hydrodynamic data (Figure 1) and of course, for all the social engineering ideas: root-beer floats, potlucks, the beard. Rebecca Ross (a.k.a Rebecca Scott) humored me. Jennifer Smith for making sure my shirt tag wasn't sticking out and showing me that Niall does graduate students. Cristina Urizar and Eli Williams for also helping me survive Aggieland. Numerous other friends for making graduate a pleasant experience – if you are reading this you need to call.

I would also like to thank the following professors in the Departments of Geography, Geology and Oceanography for their assistantships: Dr. Wormuth, Dr. Matheson, Dr. Popp, Dr. Cairns, Dr. Lafon, Dr. Smith, Commander Ed Shaar,

Finally, I must thank my family for supporting me through nine years of graduate school: Srinivas Reddy, Seshe, Vijay, and Ramana Ravula.

TABLE OF CONTENTS

LIST OF TABLES

LIST OF FIGURES

I. INTRODUCTION

Planktonic foraminifera shells are used to deduce paleoclimates, but these reconstructions depend on an understanding of how the environment influences foraminiferal abundance, distribution, and ultimately their shells (e.g. Emiliani, 1966; CLIMAP Project Members, 1976; Andreasen and Ravelo, 1997; Lea et al., 2000). New laboratory methods that allow for smaller samples, and that generate finer analytic resolutions hold promise for new discoveries (e.g., electron microprobe Nürnberg et al., 1996a&b), but may outpace our current understanding of foraminifera biology.

Early biogeographic studies revealed that the distribution of each planktonic foraminifera species is limited to the climate they have adapted to, so a species can indicate a climate types: sinistral *Globigerina pachyderma* for polar temperatures, or *Globigerinoides sacculifer* for tropical temperatures (Bé and Tolderlund, 1971). Typically, however, a whole assemblage is used to determine one of five general climate types: polar, subpolar, transition (temperate), subtropical, and tropical (Hemleben et al., 1989; Bé and Tolderlund, 1971). The occurrence of a unique species can signify climatic, seasonal or hydrographic changes such as upwelling or stratification (e.g. Peterson et al., 1991).

Because they subsist on either plankton and/or their algae symbionts, most planktonic foraminifera are found in the euphotic zone, and reflect the sea surface environment (Bé, 1982). Many migrate throughout the water column through osmotic regulation of their protoplasm controlling their density and thus depth (Savin and Douglas, 1973). Living species can migrate up to 50 m per day compared to dead

---

This thesis follows the style of *Geochimica et Cosmochimica Acta.*

specimens that descend through the mixed layer in less than a day (Hemleben et al., 1989; Takahashi and Bé, 1984). These diel migrations imply that foraminifera have adapted to adjust their depth distributions to seek a preferred water property such as temperature, density, the deep chlorophyll maximum (prey location), or another depth dependent property (Savin and Douglas 1973; Bé, 1977; Fairbanks and Wiebe, 1980). Ultimately, depth zonation facilitates algae-symbionts, prey availability, or predator avoidance.

Generally, the depth habitats are characterized as shallow, intermediate, or deep (0-50, 50-100, and >100 m respectively; Bé, 1977), although most planktonic foraminifera thought to precipitate their shells in a smaller, species-specific depth range above the thermocline (Emiliani, 1954; Fairbanks et al., 1982). At these depths, foraminifera precipitate a calcite shell whose make-up is a function of the seawater composition and temperature (Emiliani, 1955). Some species, however, can precipitate significant amounts of calcite after descending out of the mixed-layer and so their shell geochemistry poorly represents water properties at the sea surface (Rosenthal et al., 2000). Previous investigators have used these distinctions to calculate seasonal sea surface temperatures (Deuser, 1978; Williams et al., 1979; Deuser et al., 1981). Classically, $\delta^{18}O$ data is used to estimate sea surface temperature, but more recently, $\delta^{18}O$ data is interpreted to estimate past sea surface densities and salinities (Epstein et al 1951; Emiliani, 1955; Shackelton and Opdyke, 1973; Billups and Schrag 2000; Hillaire-Marcel et al., 2001). Researchers have also tried to correlate the $\delta^{13}C$ of tests to surface water structure and nutrient concentration (Williams et al., 1977; Kohfeld et al., 2000; Mortyn et al., 2002). Other researchers have correlated test major or minor element composition such as Mg, Sr, or Nd to temperature, salinity, or nutrient concentrations (Boyle, 1981; Cronblad and Malmgren, 1981; Nürnberg et al., 1996a&b; Lea et al., 1999; Vance and Burton, 1999). Depending on the species, these correlations can characterize a small depth interval across the thermocline, or may span hundreds of meters (Savin and Douglas, 1973; Fairbanks et al 1980). Because this data extracted

from a foraminifera shell reflects its habitat, knowledge of what controls this habitat is important (e.g. Spero, 1998).

Ideally, an investigator would want to take a water mass, change its properties, and see how the foraminiferal distribution and abundance are affected. In the Gulf of Mexico, circulation associated with cyclonic/anticyclonic eddies respectively raises or lowers the thermocline, changing the hydrographic properties such as temperature, nutrient concentrations, chlorophyll concentrations, etc.. By examining the surface waters in these eddies, a researcher could determine what the changes in the hydrography had on the foraminiferal abundances and distribution (e.g., Schmuker, 2000). To this end, I studied foraminifera collected from the upper 200 m at discrete depth intervals to examine their depth and species distribution through the two different environmental regimes (anticyclonic and cyclonic) to find what environmental or genetic factors control their distribution. This characterization of foraminifera distributions through the water column is relevant in ecologic studies to understand how zooplankton is distributed through the water column (Ortiz et al., 1995; Watkins et al 1996). This study also will benefit paleo-temperature reconstructions because it will answer how well a particular species characterizes sea surface temperature and climatic regimes (e.g., Fairbanks and Wiebe, 1980; Ottens, 1991; Chen and Prell, 1998).

II. OCEANOGRAPHIC SETTING AND FIELD SAMPLING

Foraminifera samples for this study were collected in the northeastern Gulf of Mexico where the circulation pattern is strongly influenced by the Loop Current. A sharp bend in this current intermittently closes upon itself forming anticyclonic eddies (Leipper, 1970; Wiseman et al., 1999). Due to their clockwise rotation and resulting convergence of waters towards their centers, the isopycnals (and so isothermals) within these eddies are depressed (Leipper, 1970). At the perimeter of the anticyclonic eddies and loop current, cyclonic eddies can also form but with elevated isopycnals due to divergence of waters from their centers (Hamilton, 1992). These cyclonic eddies tend to be 'oases' of production because divergence draws deeper, nutrient-enriched waters up to the euphotic zone; whereas anicyclonic eddies are depleted in nutrients and less productive (Biggs, 1992).

I examined planktonic foraminifera from two stations in each eddy type that were collected during a GulfCet II cruise, a Cetean census study (e.g. Wormuth et al., 2000a&b; **Table 1 and Figure 1**). Previous authors have found four stations sufficient to describe foraminifera distributions (Fairbanks et al., 1982; Ortiz et al., 1995). At each station, a Multiple Opening/Closing Net and Environmental Sensing System (MOCNESS) was used to collect the samples and hydrographic data from discrete depth intervals (Wiebe et al., 1976). The MOCNESS was towed at 1-2 knots using meter-squared, 333 μm mesh nets. Five nets were used to sample 20 m intervals from the surface to 100 m and then four nets in 25 m intervals to 200 m. The tows were collected in August at night when zooplankton are generally more abundant in surface waters. The collected plankton was rinsed out of the nets and preserved in 10% formaldehyde, 8.2 pH borate buffered solution. Depth (pressure), temperature, net angle, and the flow rate of water through the open nets were continuously recorded.

Table 1. Sampling locations, times, total biomass, and circulation regime (after Wormuth et al, 2000a).

Tow	Initial Position	Final Position	Collection Time	Integrated Biomass (cc m^{-2})	Circulation Regime
MOC1-208	26° 53.223'N 88° 24.171'W	26° 51.300'N 88° 23.158'W	21:08 - 22:50 August 6, 1997	5.6	Anticyclonic
MOC1-209	26° 48.49'N 88° 22.25'W	26° 47.16'N 88° 22.17'W	23:45 – 00:33 August 7, 1997	6.8	Anticyclonic
CTD-1		26° 0.3'N 88° 12.12'W	13:22-14:22 August 7, 1997		Anticyclonic
MOC1-217	29° 10.710'N 86° 54.803'W	29° 08.581'N 86° 54.440'W	23:06 - 00:28 August 10, 1997	8.9	Cyclonic Margin
MOC1-218	29° 04.900'N 86° 56.218'W	29° 04.598'N 86° 59.598'W	1:58 - 3:17 August 11, 1997	8.6	Cyclonic Margin
CTD-7		28° 55.0'N 87° 35.1'W	00:04-00:54 August 15, 1997		Cyclonic Margin

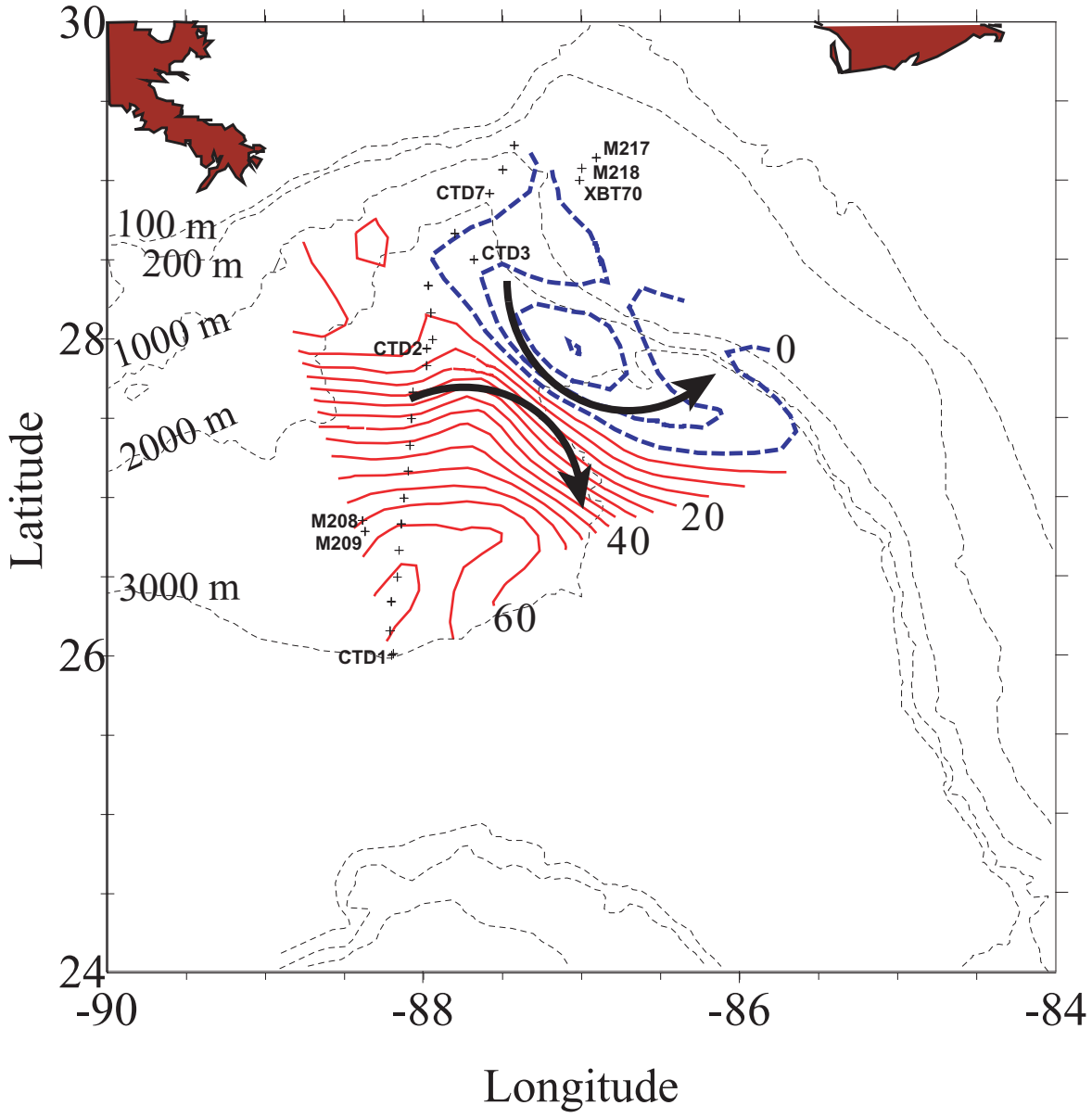

Fig. 1. Dynamic height anomaly map with station locations. Negative height (cyclone) is designated by blue dash lines; positive height (confluence and anticyclone) by red solid lines. Ciculation direction shown by arrows. (Modified figure courtesy of Joelle Ortega-Ortiz and P. Ressler).

There was no functioning conductivity sensor on the MOCNESS, thus salinity values are derived from nearby CTD casts (e.g. Zimmerman and Biggs, 1999). Comparison of the temperature profiles obtained during the MOCNESS tows and neighboring CTD casts demonstrates that the water masses are indeed the same between these stations (**Figure2**). The temperature of a MOCNESS or XBT point corresponding to the appropriate temperature interval on the CTD T-S curve was used to interpolate the salinity. Salinities calculated outside the appropriate T-S interval, using the T-S relationship of intervals 5 m above or below yielded salinities within ±0.015 psu of the values used. **Figure 3a** shows the isothermals between the location of the first CTD cast to the last MOCNESS tow. After the salinity was interpolated for the casts between the CTDs, Matlab was used to estimate the isohaline depths. The Matlab function "interp1" was used to find the depths nearest to the desired contour interval (**Figure 3b**). The error in calculated depth is estimated to be a meter or less. Isopleths of density and chlorophyll concentrations were determined in a similar fashion (**Figure 4**). Density was calculated using the UNESCO formula. Chlorophyll data was generated by an *in situ* fluorometer calibrated to CTD bottle data (**Figure 5**). The chlorophyll contours through cyclonic MOCNESS 217 and 218 were conservatively extrapolated from the values found at their neighboring CTD cast (#7) that was in close proximity and in the same environment as the tow locations, so chlorophyll profiles were likely similar (**Table 1**). To estimate the light profile, the exponential decay equation was used with typical values for August in the Gulf (**Figure 6**).

In the lab, portions of the sample were rinsed and transferred into a sorting tray filled with distilled water or alcohol. All foraminifera appeared to be in pristine condition and collected alive. Given the fast sinking times of dead species and the distinct appearance of live species, this assumption is justified (Takahashi and Bé, 1984; Watkins et al., 1996; Boltovskoy et al., 2000). When a subsample of foraminifera was tested by immersion in a rose bengal solution for the existence of test cytoplasm, all stained red, indicating protoplasm-filled specimens were collected. Every discernable foraminifera was removed from the plankton sample with a small brush and sorted by

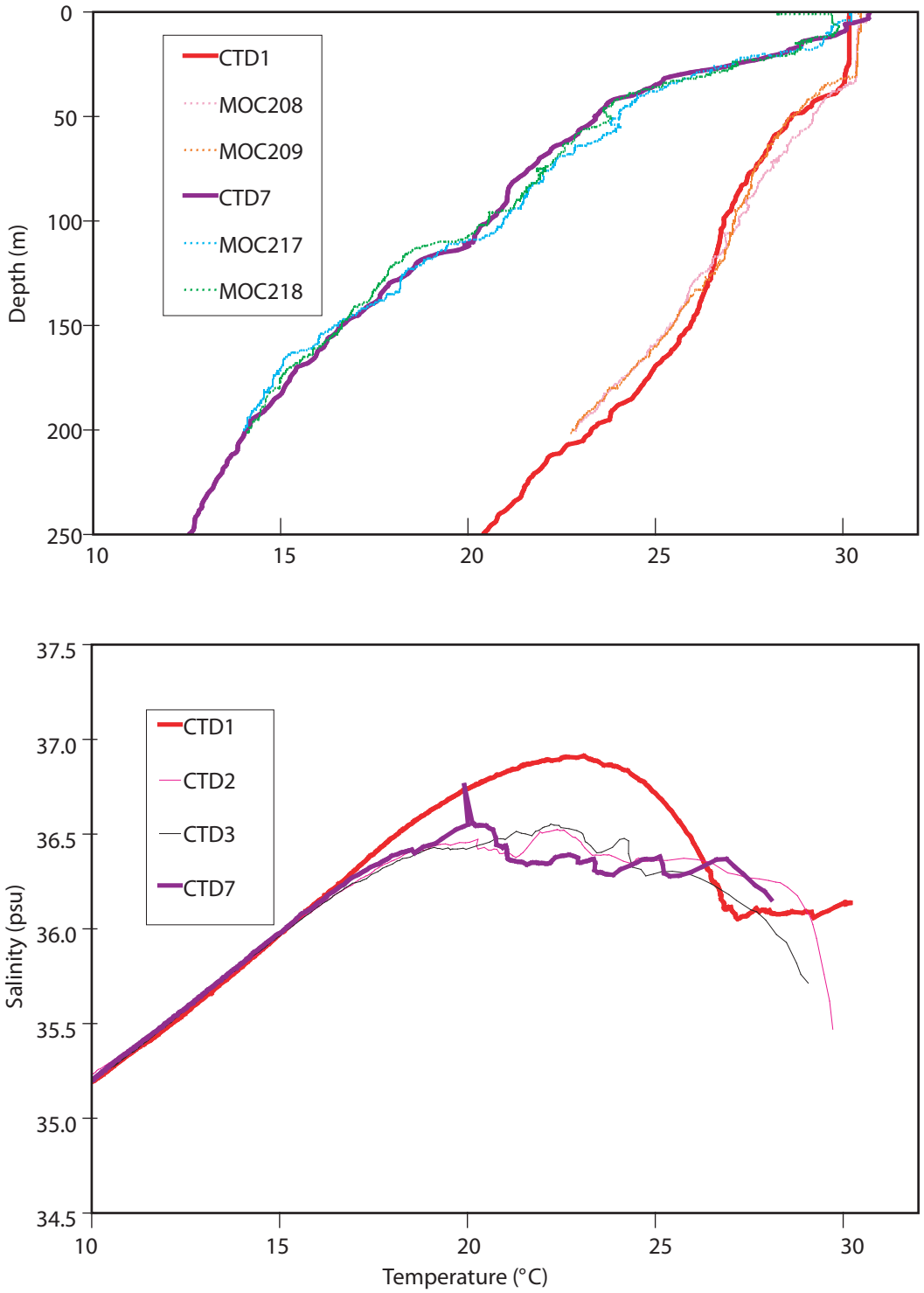

Fig. 2. (a) Temperature profiles of MOCNESS tows and the respective CTD casts used to reconstruct the MOCNESS salinity profiles. (b) The CTD temperature-salinity relationships.

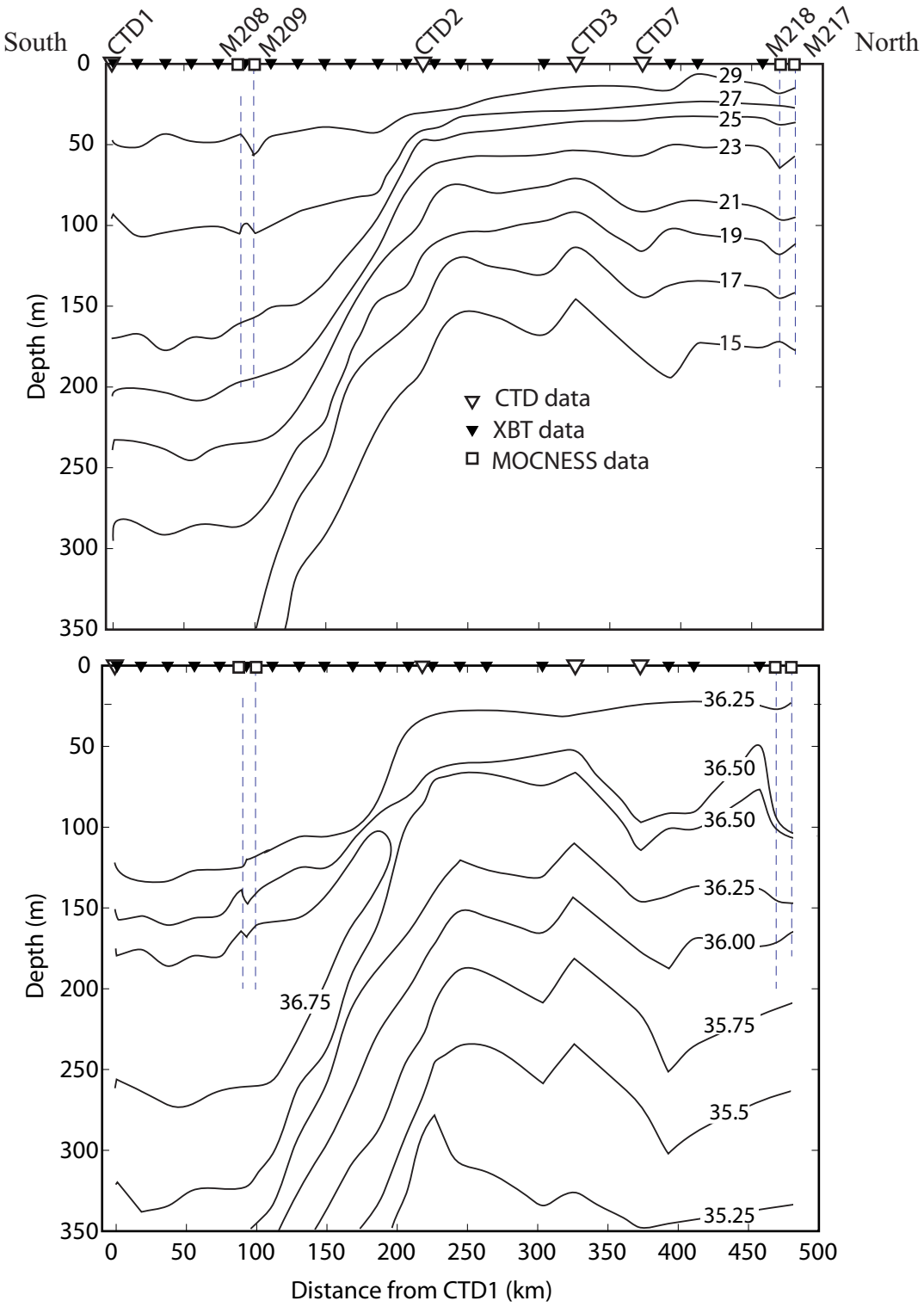

Fig. 3. (a) Isothermals (°C) along transect from CTD1 to MOCNESS 217. (b) Isohalines (psu). Dashed-dot lines represent the extent of MOCNESS data. Polygons indicate station location and source data type.

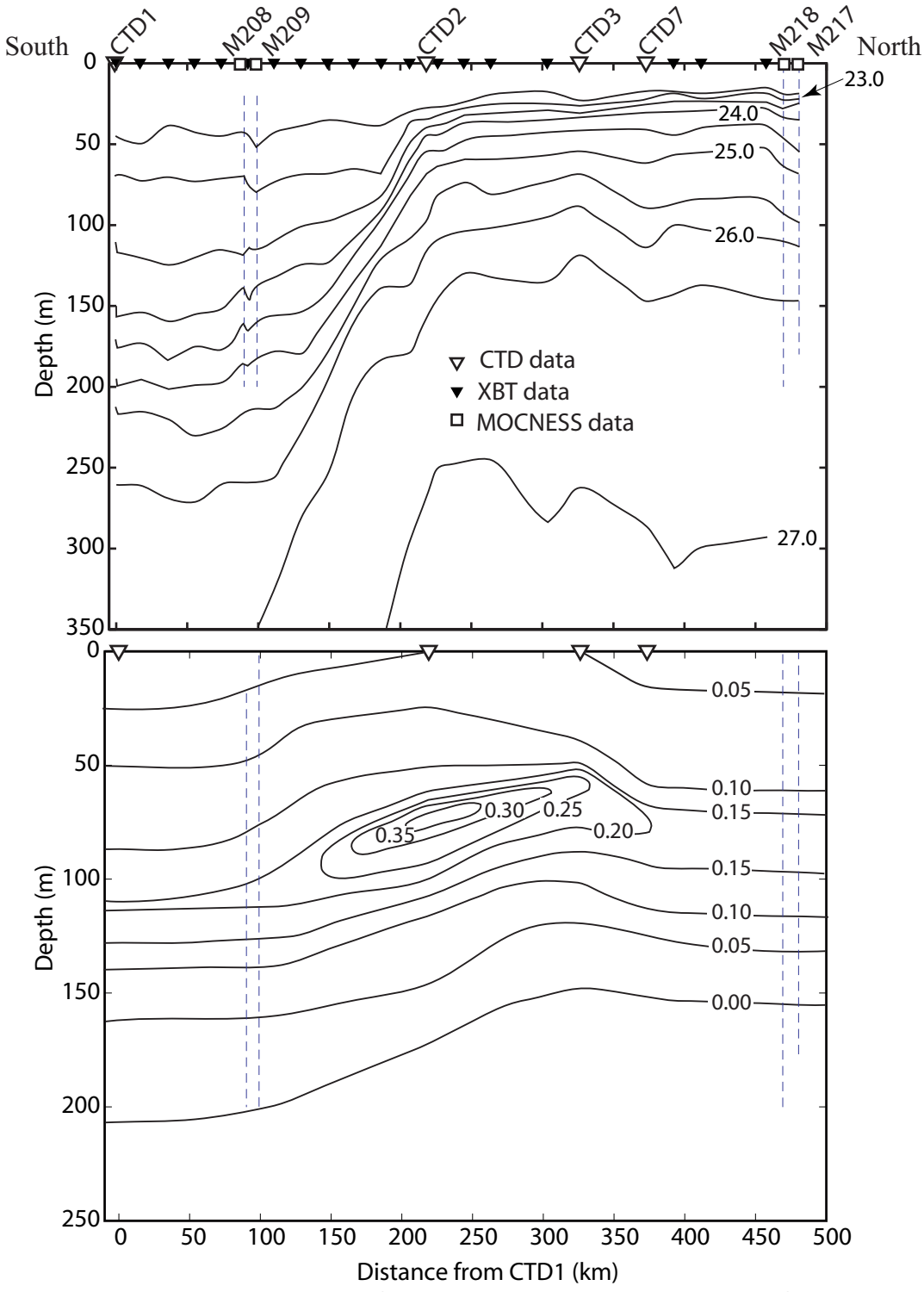

Fig. 4. (a) Isopycnals (kg/m^3). (b) Chlorophyll a concentrations (mg/m^3) between tow locations. Polygons indicate station location and source data type.

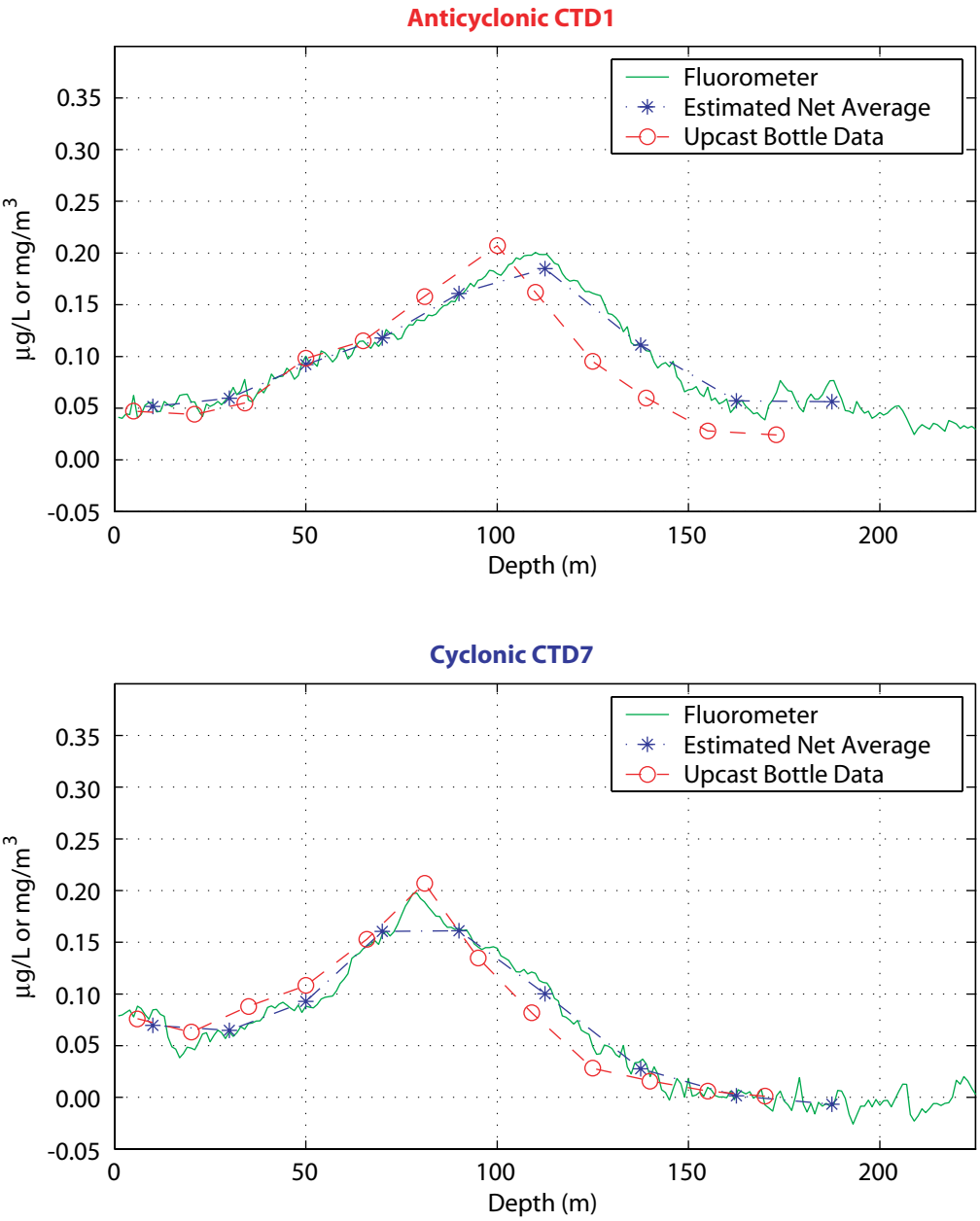

Fig. 5. CTD chlorophyll a profiles. Values are estimated to correspond to nearby MOICESS tows.

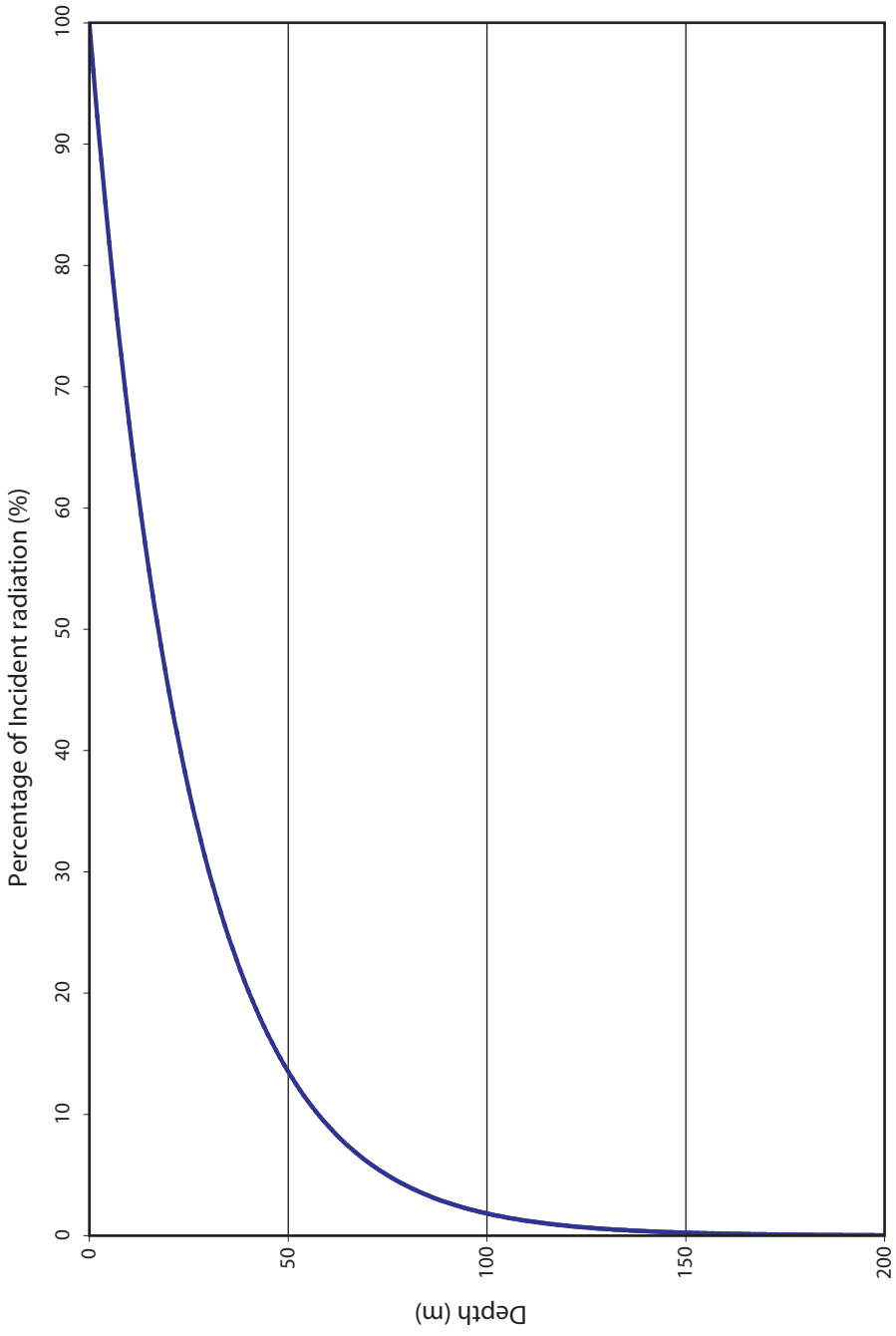

Fig. 6. Percentage of incident radiation at depth (%). Data assumes exponential decay with typical oceanic attenuation coefficient of 0.04 m^{-1}.

species onto a dry paper slide. All foraminifera were later examined with an eyepiece-mounted micrometer and individuals less than 150 μm were not considered. Species identification follows the nomenclature of Parker (1962). All plankton samples were completely examined and sorted except for the largest, the first net of MOC1-218. A one-quarter split of this sample was obtained using a Folsom plankton splitter to expedite sample analysis. Wormuth et al (2000a) determined the bulk displacement volume of zooplankton ($cc \cdot m^{-2}$) in all MOCNESS tows (**Table 1**).

Each net's foraminifera concentration (individuals m^{-3}) was determined by dividing the number of a particular species found in that net by the amount of seawater filtered by that net (**Table 2, Equation 1**). A tow's species abundance (individuals m^{-2}) was calculated by multiplying each net's species concentration by the corresponding depth interval (**Table 2, Equation 2a**) and then summing all the net values for the tow (**Table 2, Equation 2b**). This depth integrated value represents the number of foraminifera found through the entire sampled, depth interval (0 to 200 m). Percentages were calculated using the abundance values. This method normalizes each net according to the volume filtered and the depth interval towed and allows for comparison among nets (**Table 2, Equation 3&4**).

Table. 2. Equations for calculating species concentrations, abundances, and percentages

Species concentration	$=$	$\frac{\text{Number of species}_{\text{net}}}{\text{Seawater volume filtered}_{\text{net}}}$	(**Equation 1**)
Species abundance $_{net}$	$=$	$\text{Species concentration}_{\text{net}} * \text{Depth Interval}_{\text{net}}$	(**Equation 2a**)
Species abundance $_{tow}$	$=$	$\sum_{nets} \text{Species abundance}_{\text{net}}$	(**Equation 2b**)
Net foraminifera population %	$=$	$\frac{\text{Species abundance}_{\text{net}}}{\text{Species abundance}_{\text{tow}}}$	(**Equation 3**)
Tow species population %	$=$	$\frac{\text{Species abundance}_{\text{tow}}}{\sum_{species} \text{Species abundance}_{\text{tow}}}$	(**Equation 4**)
Net foraminifera property gradient	$=$	$\frac{\text{Foraminifera concentration}_{\text{net}}}{\text{Property range}_{\text{net}}}$	(**Equation 5**)

III. RESULTS AND DISCUSSION

The hydrologic character of each circulation type is distinct from the other in the upper 200 m of the MOCNESS tows with the anticyclones showing a smaller range in temperature, salinity, density, chlorophyll and nutrient concentrations. For instance, the surface temperatures for both regimes start at 30°C, but the anticyclones extend to 23°C, whereas the cyclones continue through to 14°C (**Figure 2; Figure 3a**). The warmer anticyclones also have a deeper mixed layer: about 35 m compared to 15 m, respectively. The salinity ranges and profiles between the two eddy types are also different. The anticyclonic salinities start at the surface values of 36.14 psu and increase to highs of 36.90 psu at the bottom of the tows. The cyclonic salinities do not steadily increase to the tow bottom, but start at a surface value of 33.5 and end at 35.8 psu with a shallower, smaller maximum at 110 m of 36.76 psu (**Figure 3b**). Not surprisingly like temperature and salinity, the resulting density anomalies in the anticyclones extend through a smaller range 22.0 to 25.3 in comparison to 20.1 to 26.8 $kg \cdot m^{-3}$ in the cyclones. The greater range of temperature and salinity in the cyclones and their shallower salinity peak results in a steep isohaline gradient in the upper 50 m (**Figure 4a**). With chlorophyll concentrations, both the anticyclonic and cyclonic concentrations peak at 0.20 mg/m^3, but the peak concentrations shoal from 110 m in the anticyclones to 79 m in the cyclones (**Figure 4b&5**). Corresponding nutrient data were not collected, but historically in the Gulf of Mexico nitrate concentrations become measurable at temperatures colder than 22.5°C (Biggs, 1992). The anticyclone MOCNESS tows should have no measurable nitrate beacuse this temperature occurs below the sampled interval at about 210 m. The cyclones, however, could have measurable nitrate starting at about 65 m (see **Figure 3a**). All the above differences among the MOCNESS tows result in the anticyclonic tows pairing together with nearly

identical physical properties. Likewise, the cyclonic tows pair together, however, these properties are quite distinct between the two eddy types.

Still with this marked difference between the two circulation patterns, at least 96% of the tow abundances (individuals m^{-2}) are composed of the same nine species defined in this study as common species (**Table 3&4**). Another six species found intermittently among the tows at less than 1% of the abundance are defined as rare species (**Table 3&5**). Although the surface net is missing for MOC1-208 and the last net for MOC1-218, the trends found between the circulation regimes are unaffected by these missing nets. The lowest abundances are found in the counterpart anticyclonic net of MOC1-209 and the last sampled net of MOC1-218, so estimates of the missing portions from a comparison to their counterpart nets results in at most 4% or 7% lost.[1]

Among all tows, the common species abundances (individuals m^{-2}) range considerably (**Table 4**). *G. bulloides* is either the least or most abundant ranging from 0.0 to 34.9 individuals m^{-2}. Four species have similar abundances throughout, but have higher absolute concentrations in the anticyclones and relatively more of the anticyclones: *O. universa*, *G. menardii*, *G. siphonifera,* and *G. calida* (**Table 4**). In the cyclones, three species are at least four times more abundant and result in a tripling of the total abundance: pink *G. ruber*, *G. sacculifer,* and *G. bulloides* (**Table 4**). These three species compose 65-80% of the cyclonic abundance**.** The same species contribute only 5-15% of the abundance in the anticyclonic tows. Of the remaining 15-25% of the

[1] If we assume the missing MOC1-208 net has the same composition of individuals as its counterpart, then 0.7% or 0.16 $\#m^{-2}$ were not sampled. At most, the missing portion equals the previous portion plus the greatest difference found among any of the nets (0.7%+3.7%) or 1.03 $\#m^{-2}$. Likewise for the missing net of MOCNESS 218, assuming the same portion of individuals as its counterpart, then 7.1% or 7.93 $\#m^{-2}$ were lost. This value is probably the upper limit of the missed individuals since the previously sampled net in this tow is at a minimum. For the missing anticyclone net, the missing portion is at worst about 4.4% and for the cyclonic net less than 7.1%.[1]

Table 3. Planktonic foraminifera species found in MOCNESS tows.

Common Species	Rare Species
Orbulina universa	*Globigerinoides tenellus*
Globorotalia menardii	*Globorotalia crassiformis*
Globigerinoides ruber (pink)	*Globorotalia truncatulinoides*
Globigerinoides ruber (white)	*Globorotalia ungulata*
Globigerinoides sacculifer	*Globorotalia tumida*
Hastigerina pelagica	*Globigerinoides conglobatus*
Globigerina bulloides	*Pulleniatina obliquiloculata.*
Globigerinella siphonifera	
Globigerinella calida	

Table 4. Common species tow integrated abundances (#/m^2, and **%**).

Species	MOC1-208	%	MOC209	%	MOC1-217	%	MOC1-218	%
O. universa	7.52	**21**	4.96	**21**	4.57	**7**	5.42	**5**
G. menardii	8.00	**22**	9.91	**42**	5.35	**8**	7.16	**6**
G. ruber (pink)	3.15	**9**	.36	**2**	13.06	**20**	26.41	**24**
G. ruber (white)	.17		0.00		.85	**1**	1.44	**1**
G. sacculifer	1.75	**5**	.80	**3**	7.34	**12**	26.43	**24**
H. pelagica	4.47	**12**	1.00	**4**	2.39	**4**	4.26	**4**
G. bulloides	.33	**1**	0.00		21.53	**34**	34.87	**31**
G. siphonifera	6.09	**17**	2.80	**12**	1.81	**3**	2.28	**2**
G. calida	3.88	**11**	3.68	**16**	4.53	**7**	1.45	**1**
Total (#/m^2)	35.34	**98**	23.68	**100**	61.43	**96**	109.72	**98**
Total all found (common & rare)	36.15		23.50		63.72		111.63	
Total all corrected	N/A		24.54		N/A		123.80	

Table 5. Rare species tow integrated abundances (#/m^2, and **%**).

Species	MOC1-208	%	MOC209	%	MOC1-217	%	MOC1-218	%
G. tenellus	.15	**0.4**			.11	**0.2**	.29	**0.3**
G. conglobatus					.05	**0.1**	.12	**0.1**
G. crassiformis					.21	**0.3**	.23	**0.2**
G. truncatulinoides	.21	**0.6**			.10	**0.2**	.46	**0.4**
G. obliquiloculata	.07	**0.2**					.12	**0.1**
G. ungulata	.12	**0.3**					.10	**0.1**
G. tumida	.03	**0.1**						
Unknown	.22	**.6**			1.83	**2.9**	.59	**0.5**
Total (#/m^2)	.81	**2.2**	0.0	**0.0**	2.29	**3.7**	1.92	**1.7**

cyclonic tows are four species that comprise 90% of the anticyclonic tows: *O. universa, G. siphonifera, G. calida* and *G. menardii* (**Table 4**). The distinction between anticyclonic and cyclonic regimes with respect to species abundances is statistically confirmed through principal component analysis (**Figure 7**). Using the species abundances of each tow, Statview yields two factors, 1 and 2 (**Table 6**). Factor 2 corresponds with the anticyclones (46% of variance) and Factor 1 with the cyclones (49% of the variance). Consequently, a change in the species composition is evident between the two environmental regimes (**Figure 8**).

Plots of each species percentage versus depth show this shift of dominant species and also a shift in the most abundant depth (**Figures 9 & 10**; **Table 7**). The peak abundances for the anticyclonic tows occur comparatively deeper between 100-150 m with over a quarter of the tow's population found in this depth interval (**Figure 9**). Cyclonic abundances occur shallower between 20-40 m with over a third of the tow's population (**Figure 10**). The change in the dominant foraminiferal species and in the depth of peak abundances between the two environmental regimes indicates that some depth dependent properties control their distribution in either eddy type. Also qualitatively, foraminifera without a preference for any depth dependent variable or without any depth control should appear to shoal to the surface in the upwelled cyclones. Three species do not consistently shoal to the surface as shown by their cyclonic median depths indicating that some foraminifera can control their depth and may have a preference as to where they situate in the water column (**Table 8**)[2]. Where foraminifera concentrate generally indicates the location of a water property that the species have adapted to exploit (e.g. Ortiz et al., 1995). If these peaks coincide with a depth, temperature, density, and/or chlorophyll value, a relationship with this variable is implied.

[2] The species abundances were found across depth intervals, so the reported median depths imply a greater accuracy than the collection data, but represent an estimate of where the populations reside in the water column.

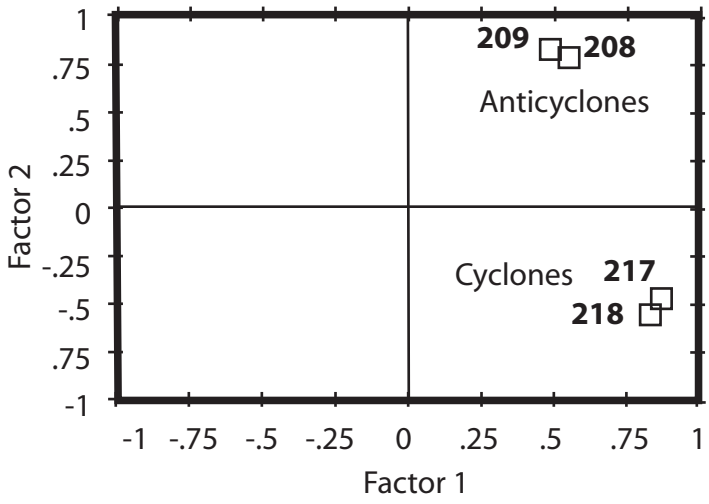

Fig. 7. Tow factor analysis results.

Table 6. Tow factor values.

Variance	.491	.459
Tow	Factor 1	Factor 2
MOCNESS 208	.546	.797
MOCNESS 209	.485	.836
MOCNESS 217	.872	-.453
MOCNESS 218	.820	-.543

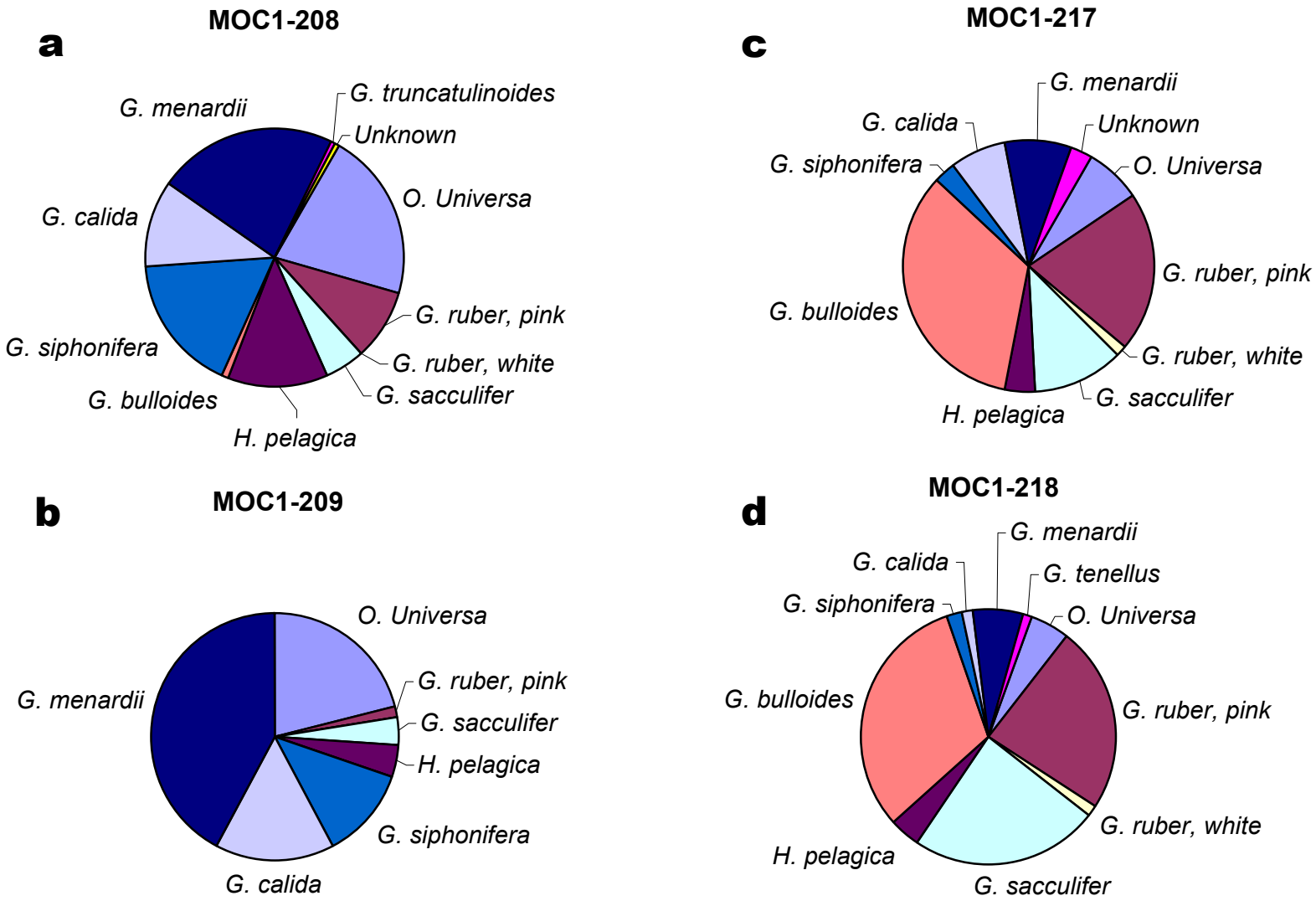

Fig. 8. Tow species compositions (%). Left **a** & **b**: anticyclones. Right **c** & **d**: cyclones.

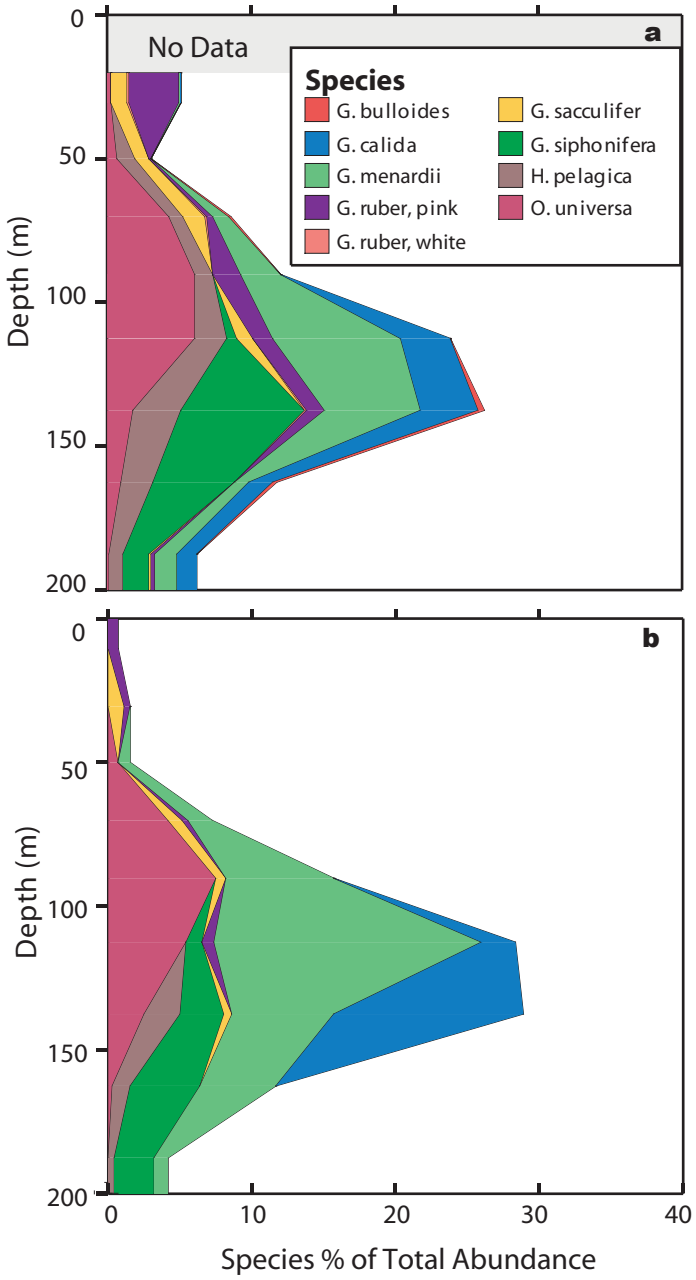

Fig. 9. Anticyclonic tow abundances (%). (**a**) Species Composition of MOC1-208. (**b**) Species Composition of MOC1-209. Data points are at each net center and are the species abundances (#m^{-2}) divided by tow total (#m^{-2}) . Points at the tow boundaries are extapolated to the nearest net center's values.

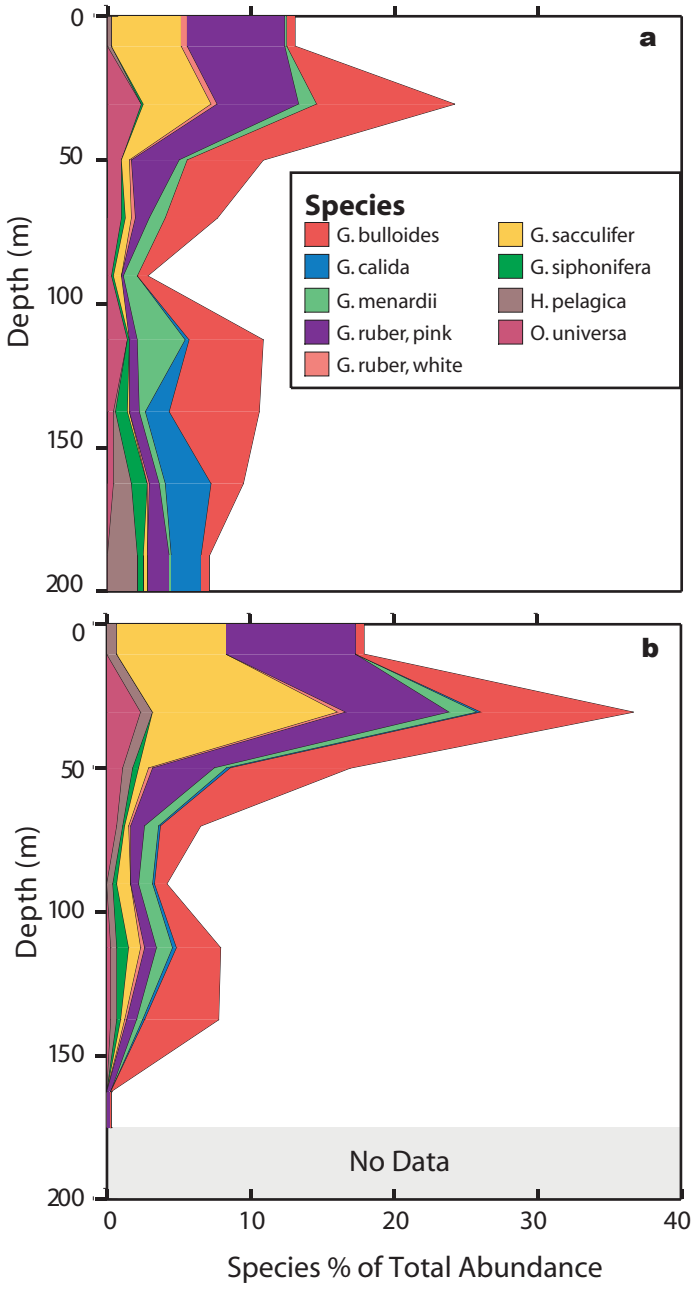

Fig. 10. Cyclonic tow abundances (%). (**a**) Species Composition of MOC1-217. (**b**) Species Composition of MOC1-218. Data points are at each net center and are the species abundances (#m^{-2}) divided by tow total (#m^{-2}) . Points at the tow boundaries are extapolated to the nearest net center's values.

Table 7. Tow foraminifera percentage at each depth interval. (Bold numbers represent peak concentrations.)

	Anticyclonic		Cyclonic	
Depth range (m)	MOC208	MOC209	MOC217	MOC218
0-20	N/A	0.7	13.0	18.0
20-40	5.3	1.6	**24.1**	**36.7**
40-60	3.1	1.6	10.9	17.0
60-80	8.7	7.2	7.6	6.5
80-100	12.2	15.7	2.7	4.2
100-125	**23.9**	**28.3**	10.9	7.9
125-150	**26.3**	**28.9**	10.5	7.8
150-175	11.9	11.7	9.5	0.3
175-200	6.3	4.2	7.1	N/A

Table 8. Species median depth (m) per tow. *Denotes bimodal species distribution.

Species	MOC1-208	MOC209	MOC1-217	MOC1-218
O. universa	96	94	63	41
G. menardii	120	115	101	65
G. ruber (pink)	84*	39	32	28
G. ruber (white)	77*	N/A	29	52
G. sacculifer	65*	70	24	26
H. pelagica	128	146	177	55
G. bulloides	142*	N/A	69	51
G. siphonifera	147	159	153	104
G. calida	136	135	164	81

Statistical analysis of the foraminifera species and their tow abundances yields two factors (discussed in further detail below). Factor 1 accounts for 62%, factor 2 28% of the variance among species abundance (**Table 9**). Six species have a factor 1 value greater than .9: pink and white *G. ruber, G. sacculifer, G. bulloides, G. conglobatus,* and *G. crassiformis*. Three other species have a factor 2 value greater than .9: *H. pelagica*, *G. tenellus,* and *G. truncatulinoides* (**Table 9**). Five species have a factor 1 value that was around -.75: *O. universa, G. siphonifera, G. menardii, P. obliquiloculata, G. ungulata,* and *G. tumida*. Two species *G. menardii* and *O. universa* share nearly identical factor 1 values, but their factor 2 values are of opposing signs, isolating *G. menardii* in its own region. Likewise, *G. siphonifera* and *G. calida* share similar Factor 2 values, but their factor 1 values are also inverted (**Figure 11**). To see what these factors correspond to, a comparison was made among several water properties and the corresponding species abundances.

Because chlorophyll maximum shoals like the species concentrations in the cyclones, it seems a likely candidate to correspond to factor 1 or 2 (**Figure 5**). For the anticyclonic tows, the maximum percentage of foraminifera coincides with the chlorophyll peak at 110 m (**Table 7**; **Figure 9**). This correlation is primarily due to the largest component of the anticyclonic abundance, *O. universa* and *G. menardii*, peaking with the chlorophyll maximum. For the cyclonic tows, the peak foraminifera abundances occur at a depth of 20-40 m which does not correspond to the chlorophyll maximum at ~80 m (**Table 7**; **Figure 10**). In the cyclones, the lowest foraminifera concentrations coincide with the highest chlorophyll concentrations. The foraminifera abundances peak at a low chlorophyll concentration of 0.08 mg/m^3. Scatter plots of the each species concentration versus the chlorophyll concentration yield poor correlation coefficients (**Figure 12**). Only *O. universa* and *G. menardii* hint at a correlation in the anticyclonic tows with the highest correlation coefficients of 0.86 and 0.79. In the anticyclones, a better correlation is expected beacuse the peak abundances and chlorophyll maximum seem to coincide. Even more surprising, an inverse relationship between foraminifera concentrations and chlorophyll is found in the cyclones. In both

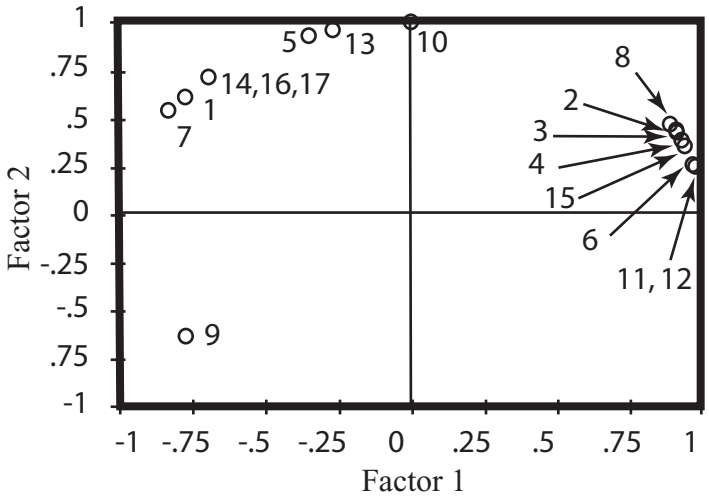

Fig. 11. Species factor analysis results.
Numbers correspond to species indicated in Table 9.

Table 9. Species factor values.

	Variance	.620	.280
	Species	Factor 1	Factor 2
1	*Orbulina universa*	-.777	.630
2	*Globigerinoides ruber (pink)*	.904	.428
3	*Globigerinoides ruber (white)*	.909	.418
4	*Globigerinoides sacculifer*	.930	.369
5	*Hastigerina pelagica*	-.350	.937
6	*Globigerina bulloides*	.967	.253
7	*Globigerinella siphonifera*	-.835	.550
8	*Globigerinella calida*	.889	.457
9	*Globorotalia menardii*	-.781	-.624
10	*Globigerinoides tenellus*	-.003	1.00
11	*Globigerinoides conglobatus*	.971	.240
12	*Globorotalia crassiformis*	.971	.240
13	*Globorotalia truncatulinoides*	-.272	.962
14	*Pulleniatina obliquiloculata.*	-693	.721
15	Unknown	.938	.347
16	*Globorotalia ungulata*	-.693	.721
17	*Globorotalia tumida*	-.693	.721

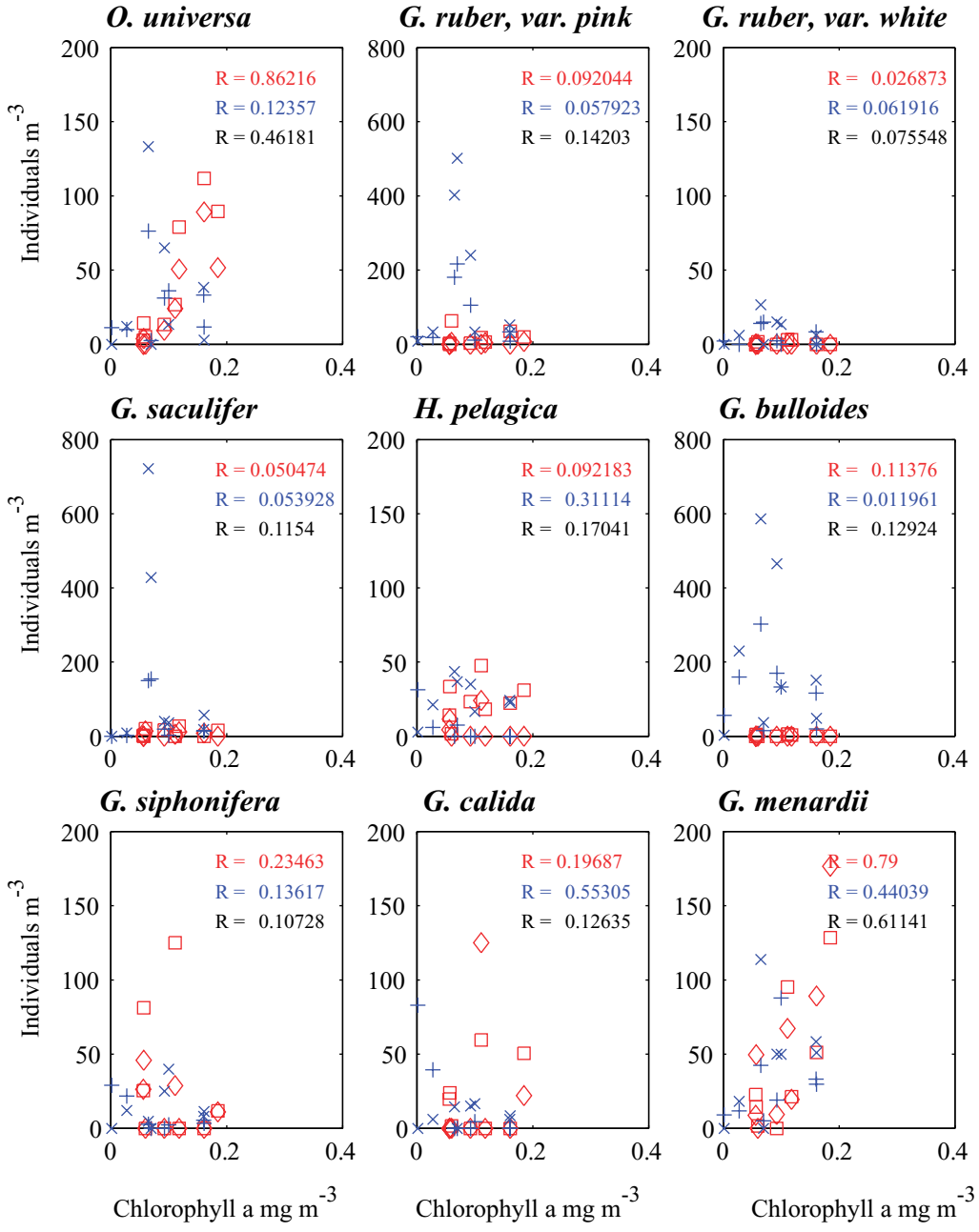

Fig. 12. Scatter plot of each species versus chlorophyll concentrations. The least squares regression coefficient for all regimes is given in black, in red for only the anticyclonic data, and in blue for only the cyclonic data. Red square and diamonds represent MOC1-208 and MOC1-209. Blue plus sign and x marks represent MOC1-217 and MOC218, respectively.

eddy types, the presence of nitrate also does not correlate with the abundance peaks. The anticyclonic abundance peaks at least 60 m shallower than when nitrate concentrations first appear at 210 m. For the cyclones, the nitrate maximum at 65 m is next to the abundance minimum (**Table 7**). Neither factor 1 nor 2 corresponds directly to chlorophyll or nitrate. The weak correlation of chlorophyll suggests that although it may not directly correspond to factor 1 or 2, it may correspond to one of these factors in combination with another property.

For each tow, the concentration of each species against depth, temperature, and density was examined to see how these hydrographic factors controlled the foraminifera distribution. The depth profiles are shown by species in **Figures 13a-21a**. The area of each bar is the integrated number of individuals found at the sampled interval ($\#m^{-2}$/net). Six species shoal at shallower depths in cyclonic conditions: *O. universa, G. menardii*, pink *G. ruber,* white *G. ruber, G. sacculifer,* and *G. bulloides* (**Table 8**). Two other species show similar distributions in the first three tows: *G. siphonifera,* and *G. calida*. One species shows no recognizable pattern among the tows: *H. pelagica*.

To show the effect of temperature and density on the abundances, the shape of the depth profiles were transformed to show the vertical concentration gradients for each species versus temperature and density (**Figures 13b,c - 21b,c**). The width of the bars is the temperature or the density range found in the net (e.g., 28.5° to 24.5°C). The horizontal axis of each bar is thus the average value found in the net (e.g., 26.5°C). The height of the bars is the abundance per the temperature or density range found across the net ($\#m^{-2}\ °C^{-1}net^{-1}$ or $\#m^{-2}\sigma^{-1}net^{-1}$). The resultant area of each bar represents the abundance ($\#m^{-2}$) found in a respective net. The shape indicates how concentrated the species are in the net. Species with tall and narrow peaks represent high concentrations in narrow property ranges, whereas short, wide bars represent abundances dispersed across a larger temperature or density range. The same peak, if found among all the tows, would represent a definite species preference for that the particular property value.

A comparison among these profiles suggests three patterns that seven of the nine common species follow: *O. universa,* and *G. menardii;* white *G. ruber,* pink *G. ruber,*

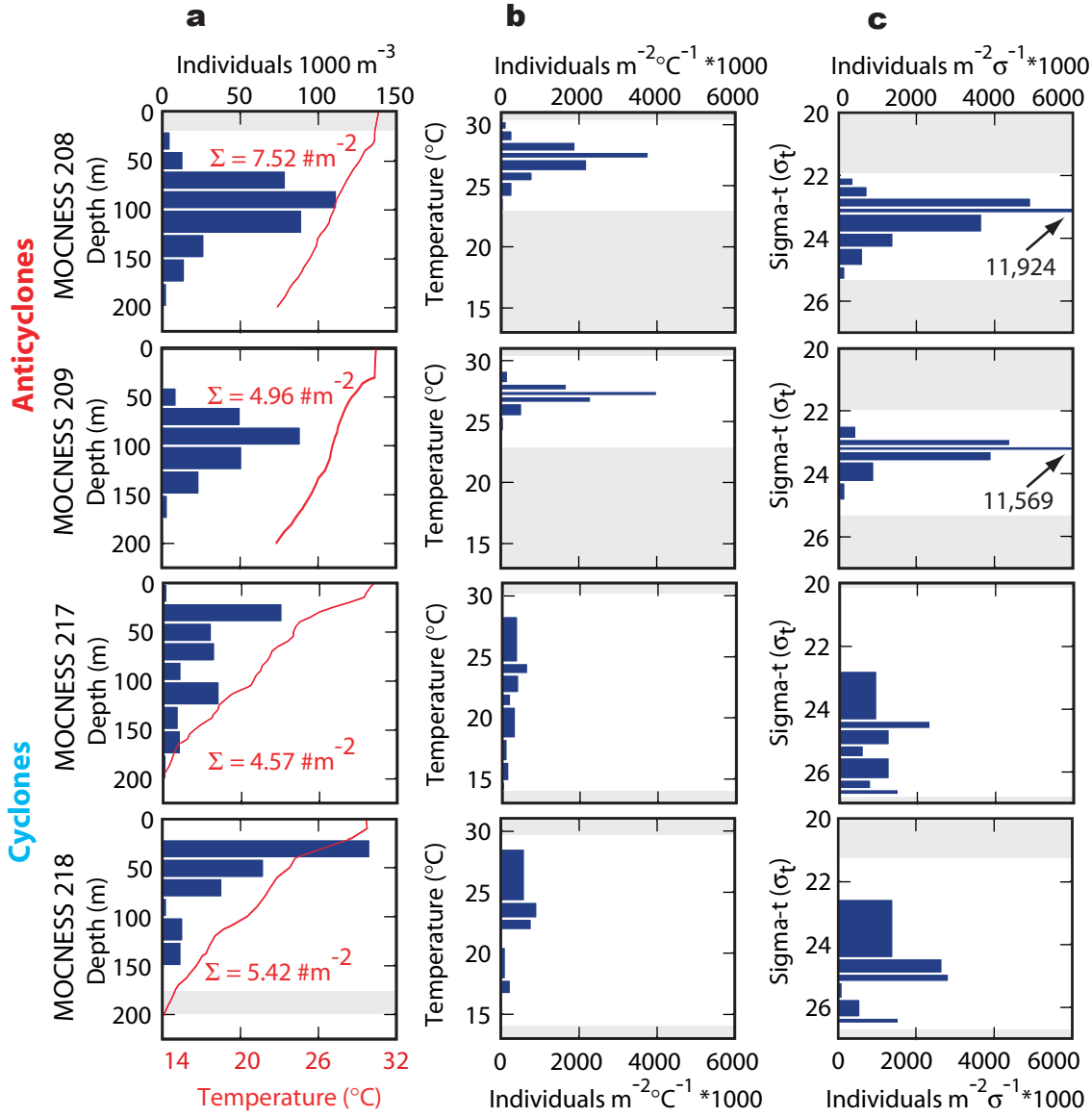

Fig. 13. *O. universa* property profiles. Column **a**: concentration (# 1000 m^{-3}) with temperature profile in red. Column **b**: temperature (# 1000 $m^{-2}°C^{-1}$). Each bar's width represents the temperature range found in the particular net. The height is the net's foraminifera abundance divided by the temperature range through the net, likewise, column **c**: density (# 1000 $m^{-2}\sigma^{-1}$). The resulting net areas integrate the same abundance shown in the corresponding net area of column **a**. Integrated tow abundances given in red. Gray shaded areas represent areas without data.

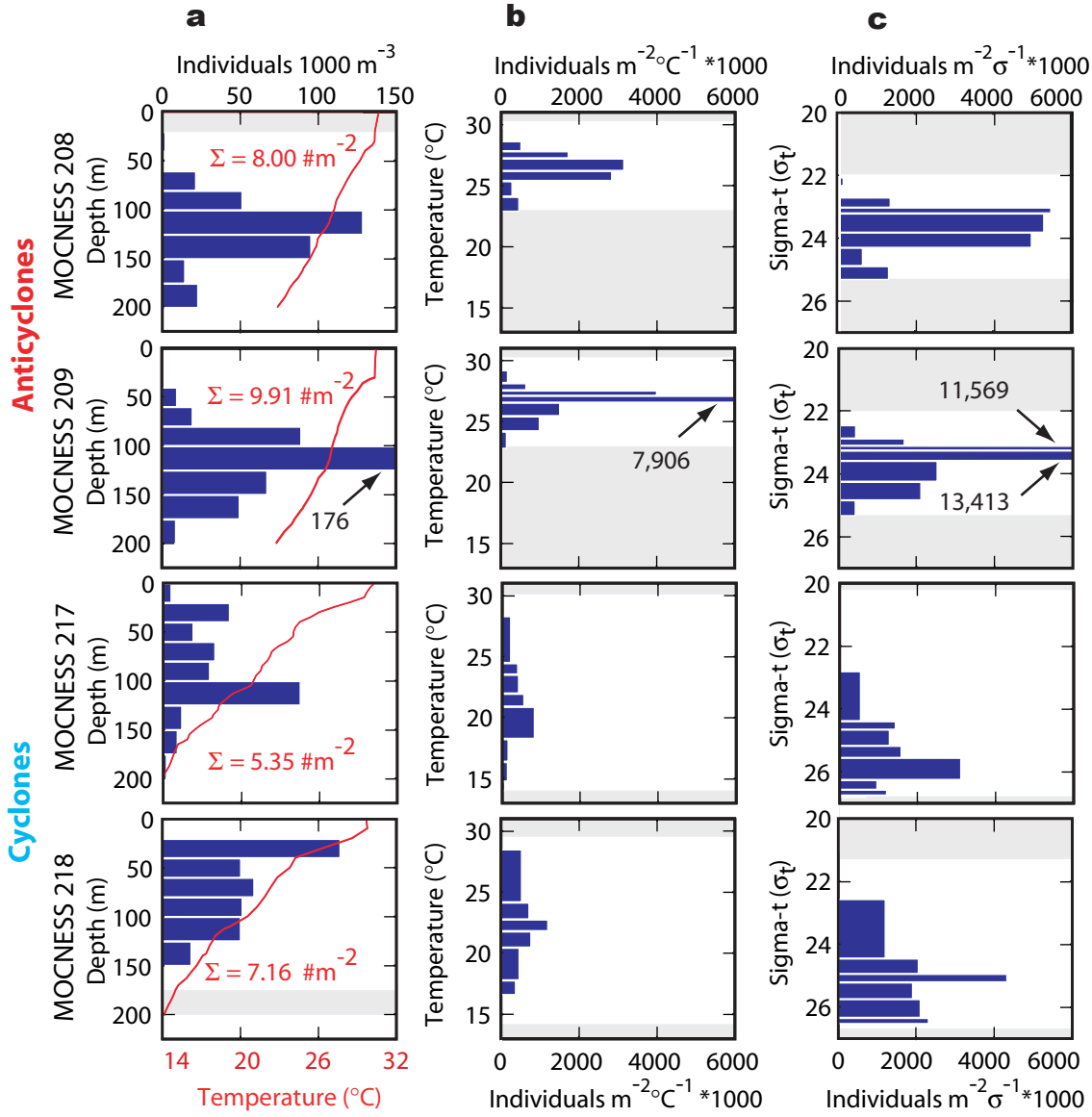

Fig. 14. *G. menardii* property profiles. Column **a**: concentration (# 1000 m^{-3}) with temperature profile in red. Column **b**: temperature (# 1000 $m^{-2}°C^{-1}$). Each bar's width represents the temperature range found in the particular net. The height is the net's foraminifera abundance divided by the temperature range through the net, likewise, column **c**: density (# 1000 $m^{-2}\sigma^{-1}$). The resulting net areas integrate the same abundance shown in the corresponding net area of column **a**. Integrated tow abundances given in red. Gray shaded areas represent areas without data.

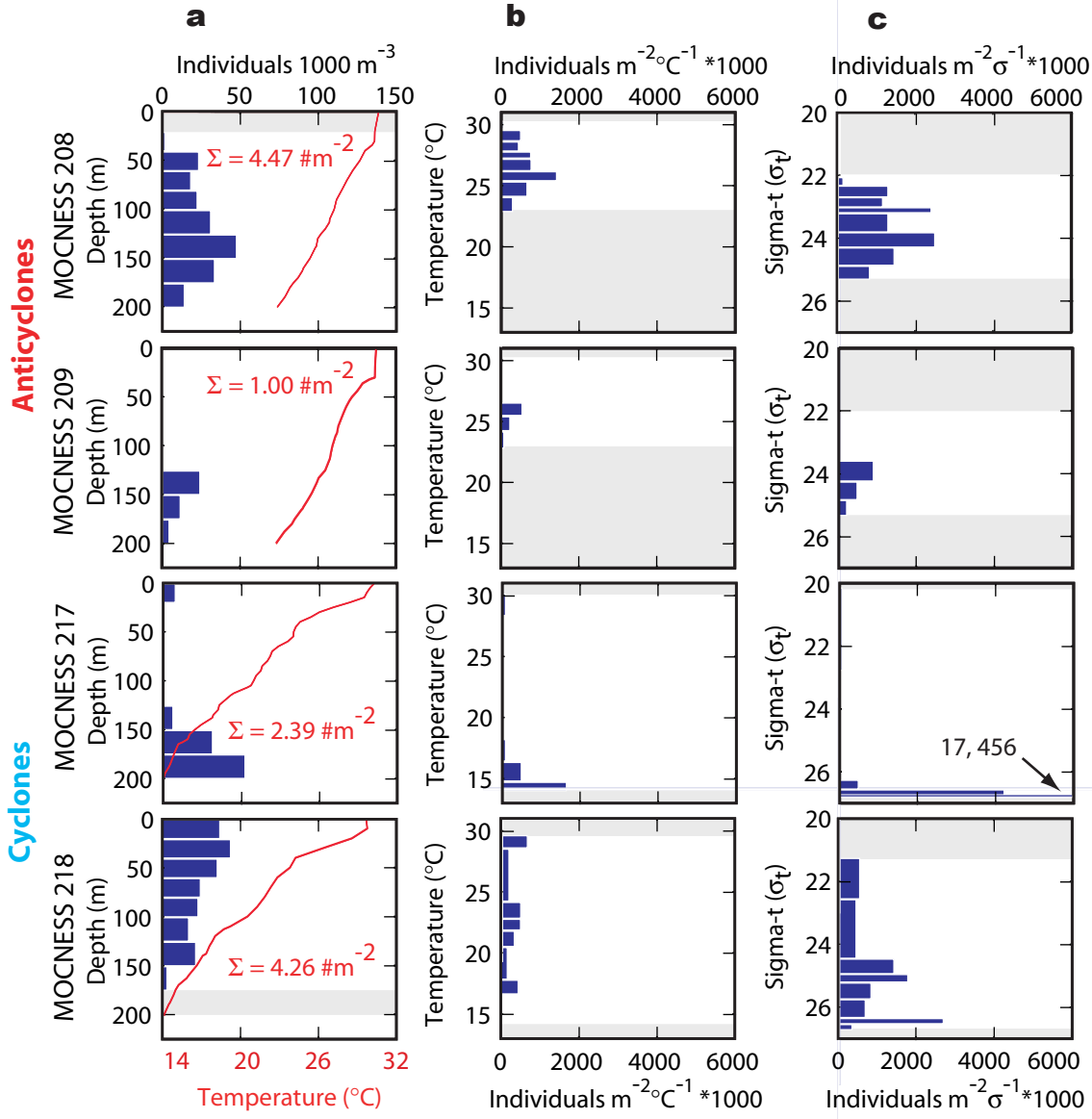

Fig. 15. *H. pelagica* property profiles. Column **a**: concentration (# 1000 m^{-3}) with temperature profile in red. Column **b**: temperature (# 1000 $m^{-2}°C^{-1}$). Each bar's width represents the temperature range found in the particular net. The height is the net's foraminifera abundance divided by the temperature range through the net, likewise, column **c**: density (# 1000 $m^{-2}\sigma^{-1}$). The resulting net areas integrate the same abundance shown in the corresponding net area of column **a**. Integrated tow abundances given in red. Gray shaded areas represent areas without data.

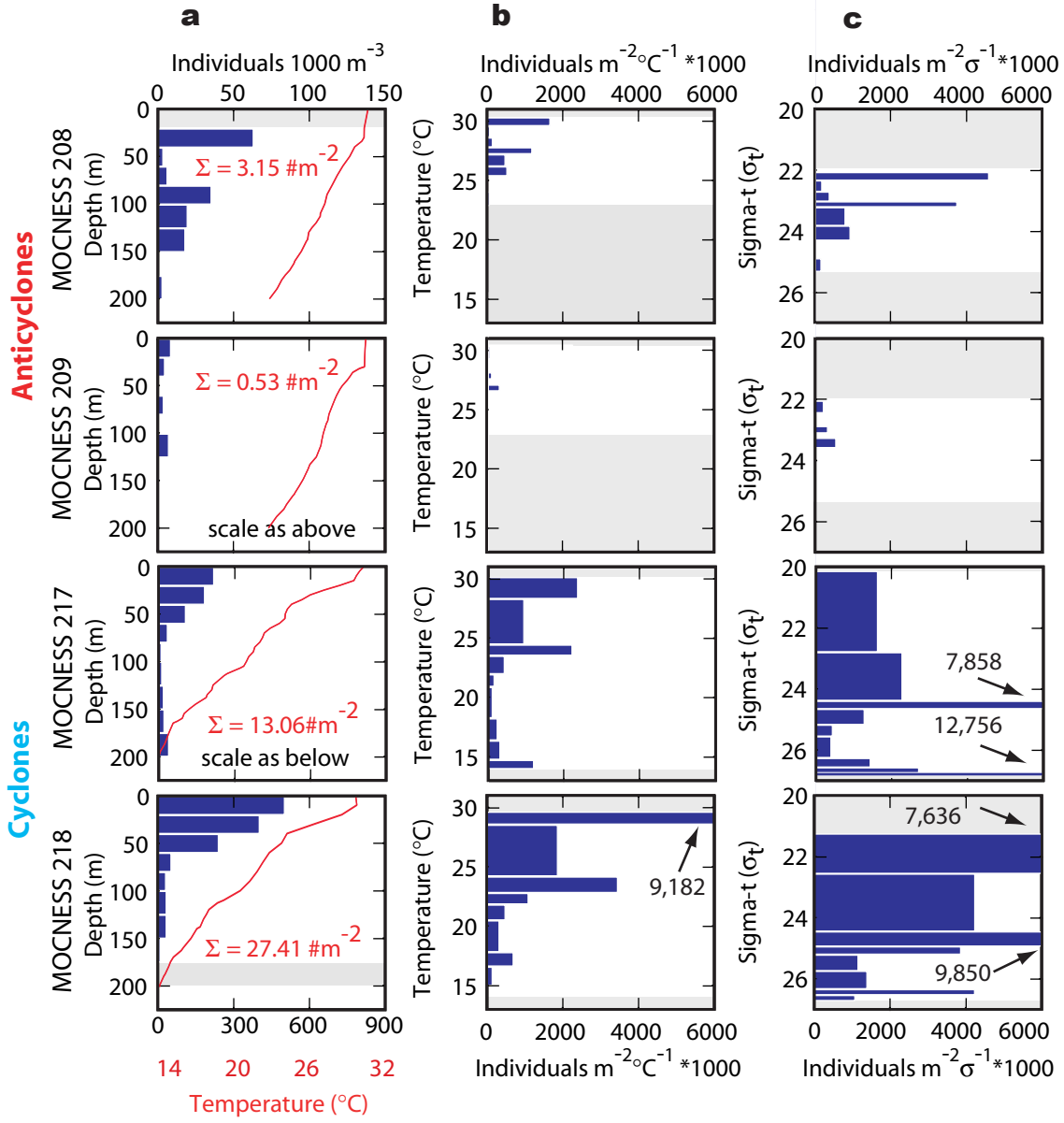

Fig. 16. *G. ruber* (pink) property profiles. Column **a**: concentration (# 1000 m^{-3}) with temperature profile in red. Column **b**: temperature (# 1000 $m^{-2}°C^{-1}$). Each bar's width represents the temperature range found in the particular net. The height is the net's foraminifera abundance divided by the temperature range through the net, likewise, column **c**: density (# 1000 $m^{-2}\sigma^{-1}$). The resulting net areas integrate the same abundance shown in the corresponding net area of column **a**. Integrated tow abundances given in red. Gray shaded areas represent areas without data.

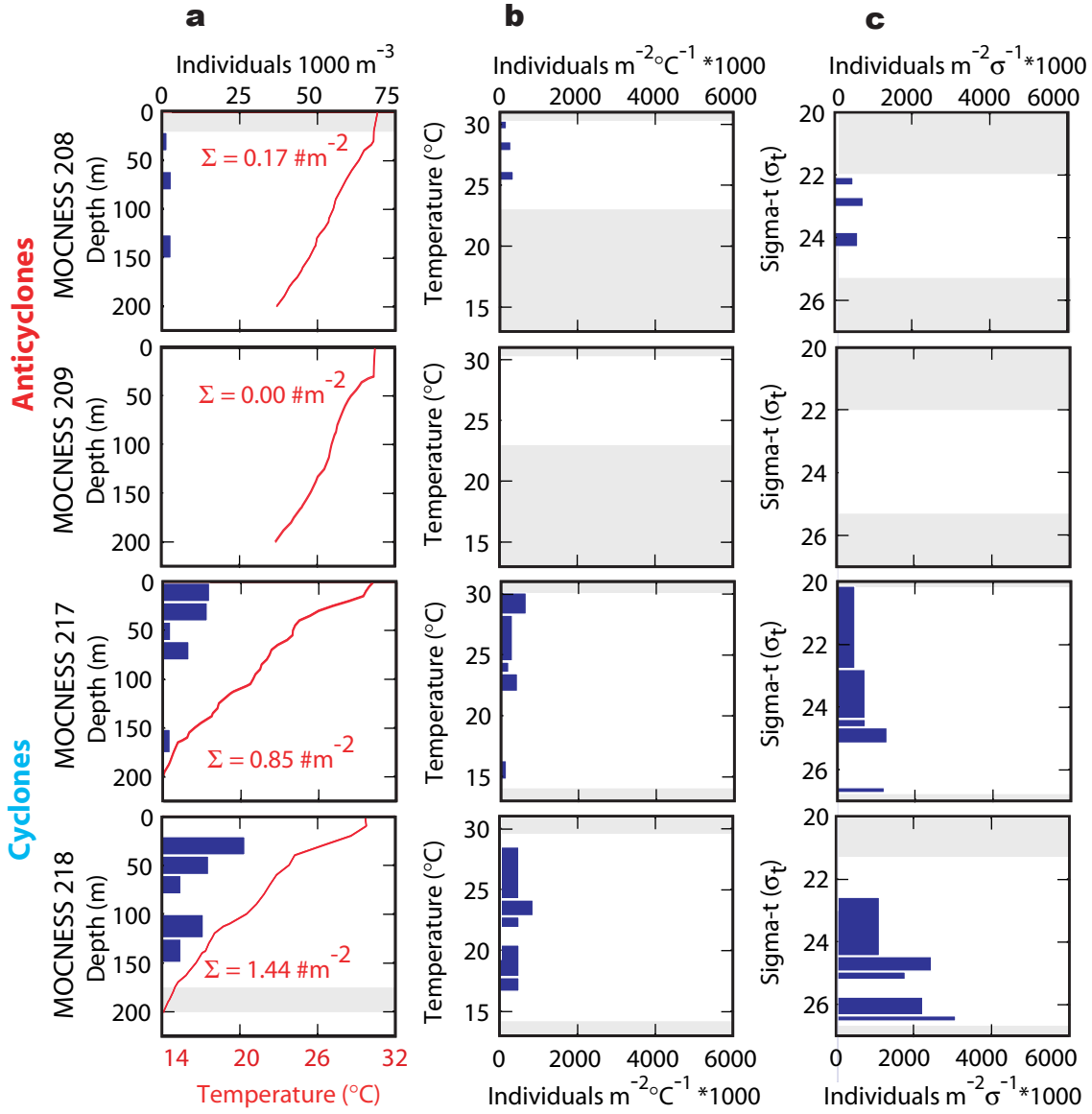

Fig. 17. *G. ruber* (white) property profiles. Column **a**: concentration (# 1000 m^{-3}) with temperature profile in red. Column **b**: temperature (# 1000 $m^{-2}°C^{-1}$). Each bar's width represents the temperature range found in the particular net. The height is the net's foraminifera abundance divided by the temperature range through the net, likewise, column **c**: density (# 1000 $m^{-2}\sigma^{-1}$). The resulting net areas integrate the same abundance shown in the corresponding net area of column **a**. Integrated tow abundances given in red. Gray shaded areas represent areas without data.

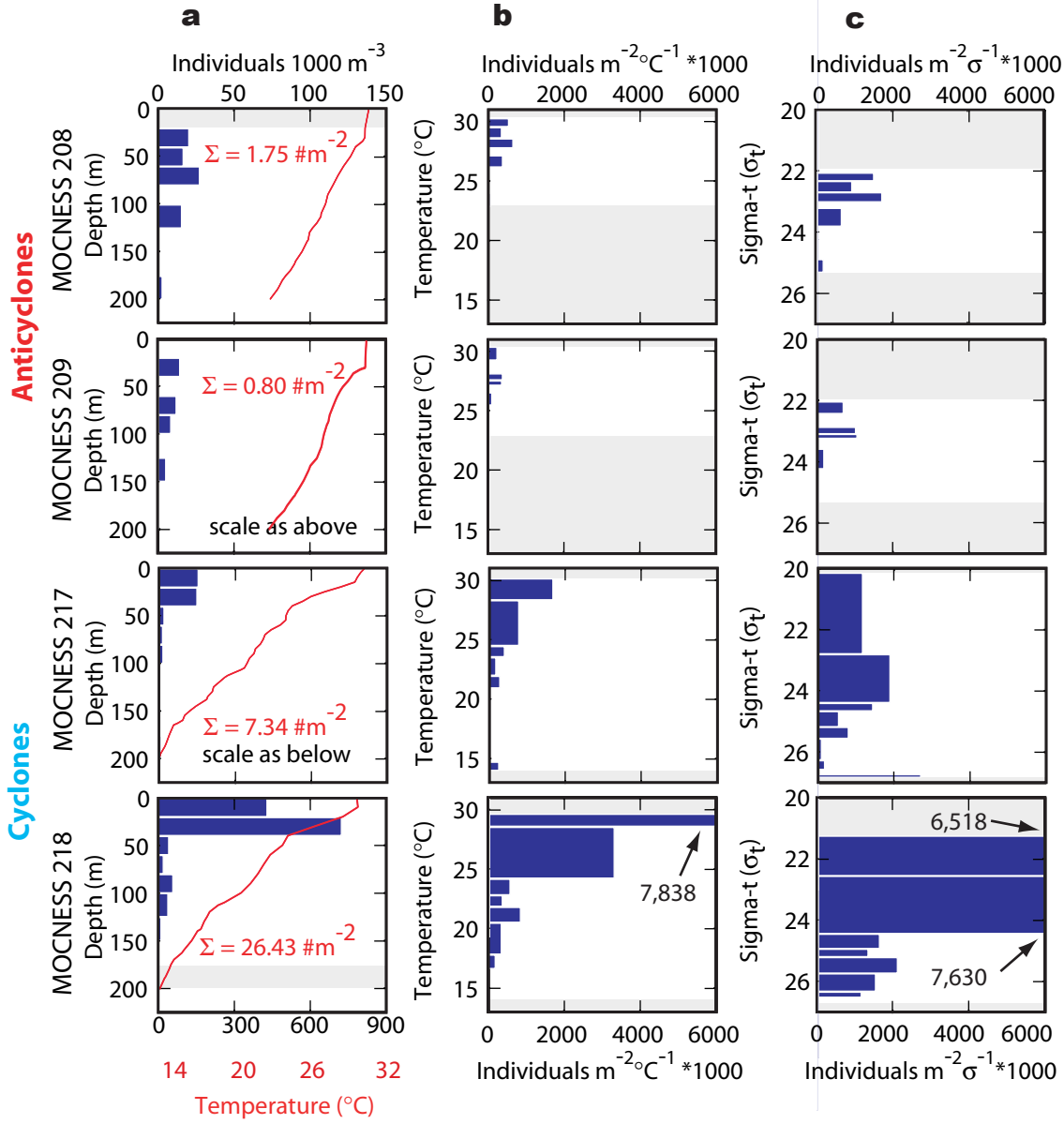

Fig. 18. *G. sacculifer* property profiles. Column **a**: concentration (# 1000 m^{-3}) with temperature profile in red. Column **b**: temperature (# 1000 $m^{-2}°C^{-1}$). Each bar's width represents the temperature range found in the particular net. The height is the net's foraminifera abundance divided by the temperature range through the net, likewise, column **c**: density (# 1000 $m^{-2}\sigma^{-1}$). The resulting net areas integrate the same abundance shown in the corresponding net area of column **a**. Integrated tow abundances given in red. Gray shaded areas represent areas without data.

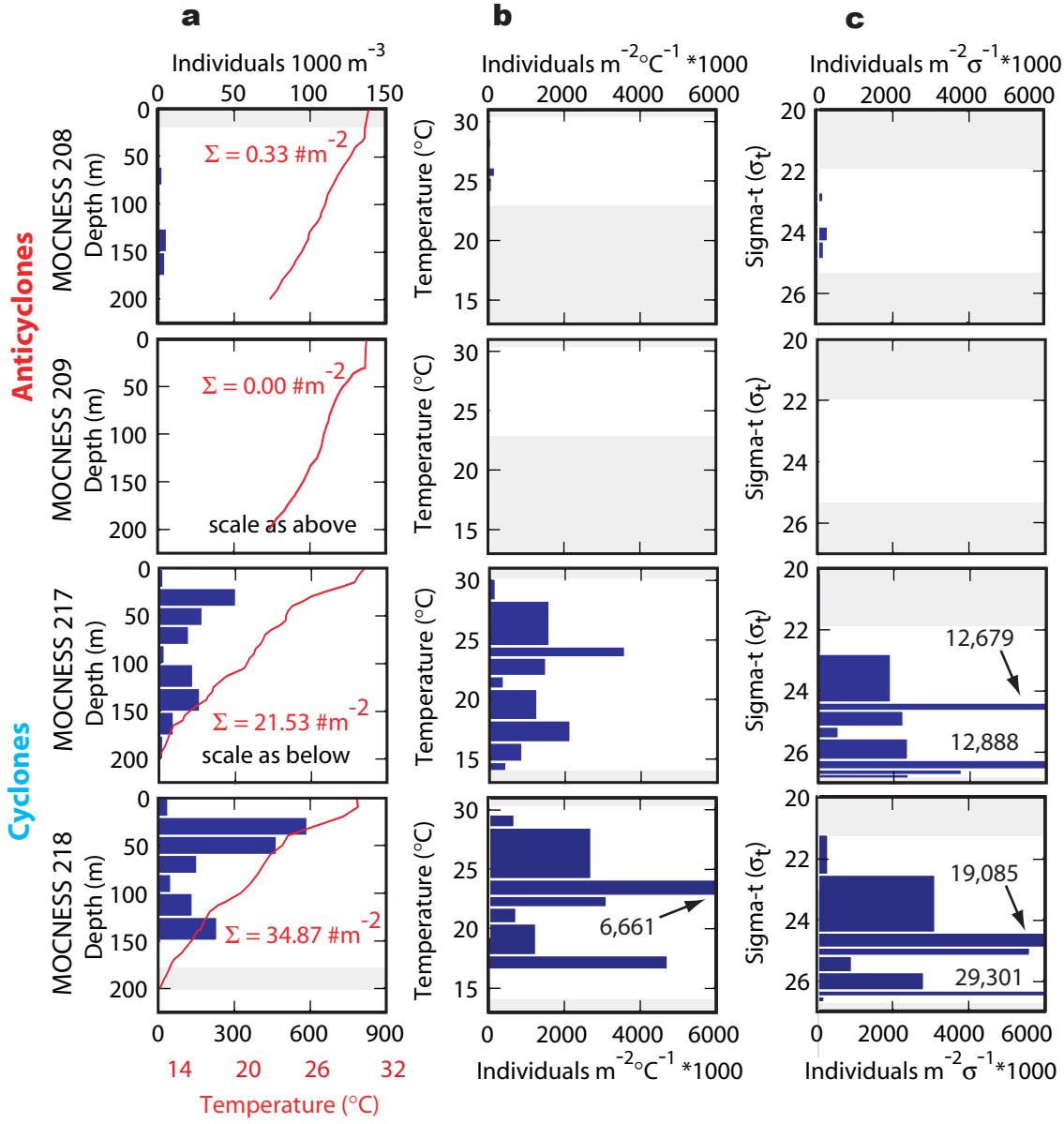

Fig. 19. *G. bulloides* property profiles. Column **a**: concentration (# 1000 m^{-3}) with temperature profile in red. Column **b**: temperature (# 1000 $m^{-2}°C^{-1}$). Each bar's width represents the temperature range found in the particular net. The height is the net's foraminifera abundance divided by the temperature range through the net, likewise, column **c**: density (# 1000 $m^{-2}\sigma^{-1}$). The resulting net areas integrate the same abundance shown in the corresponding net area of column **a**. Integrated tow abundances given in red. Gray shaded areas represent areas without data.

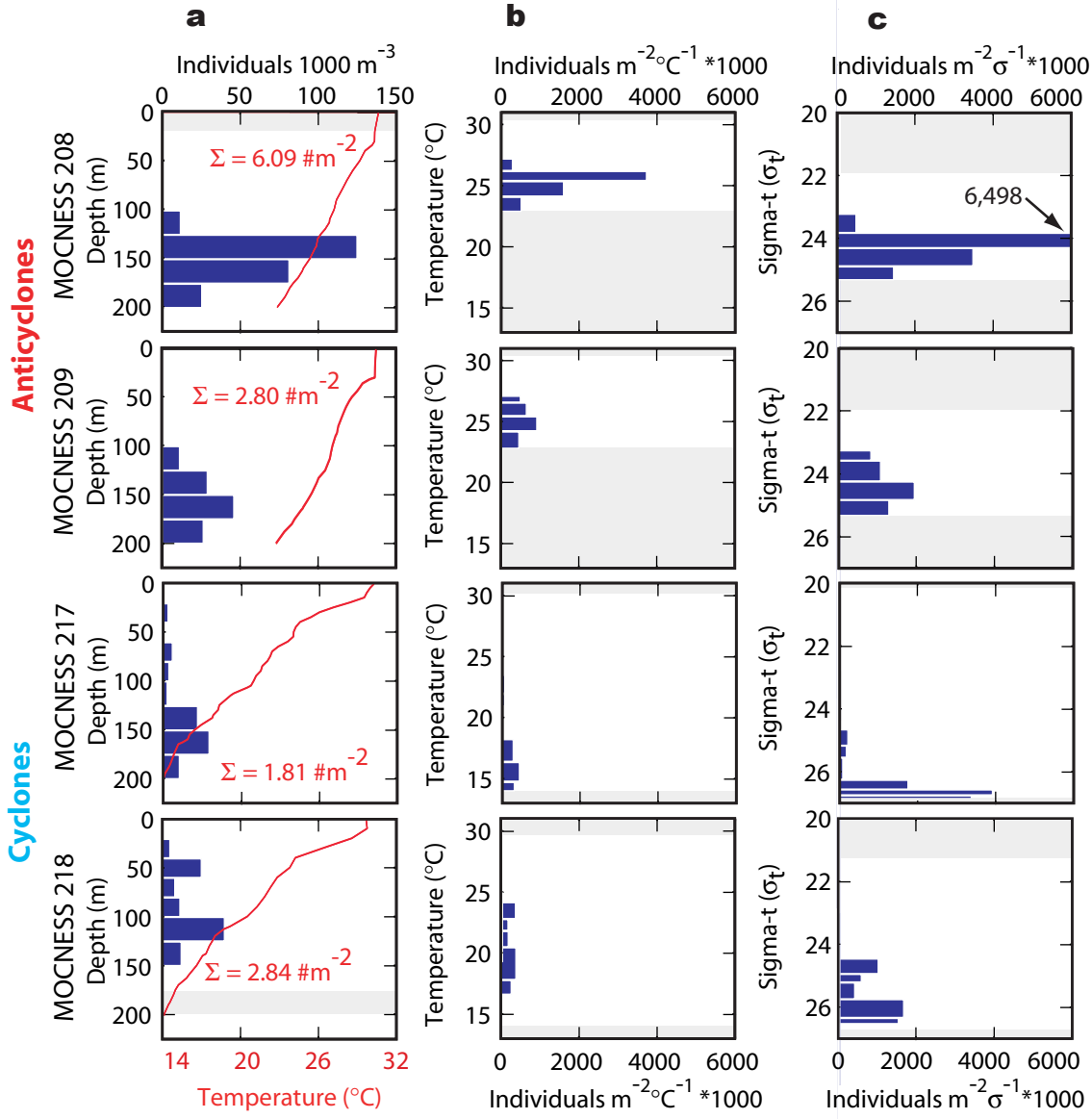

Fig. 20. *G. siphonifera* property profiles. Column **a**: concentration (# 1000 m^{-3}) with temperature profile in red. Column **b**: temperature (# 1000 $m^{-2}°C^{-1}$). Each bar's width represents the temperature range found in the particular net. The height is the net's foraminifera abundance divided by the temperature range through the net, likewise, column **c**: density (# 1000 $m^{-2}\sigma^{-1}$). The resulting net areas integrate the same abundance shown in the corresponding net area of column **a**. Integrated tow abundances given in red. Gray shaded areas represent areas without data.

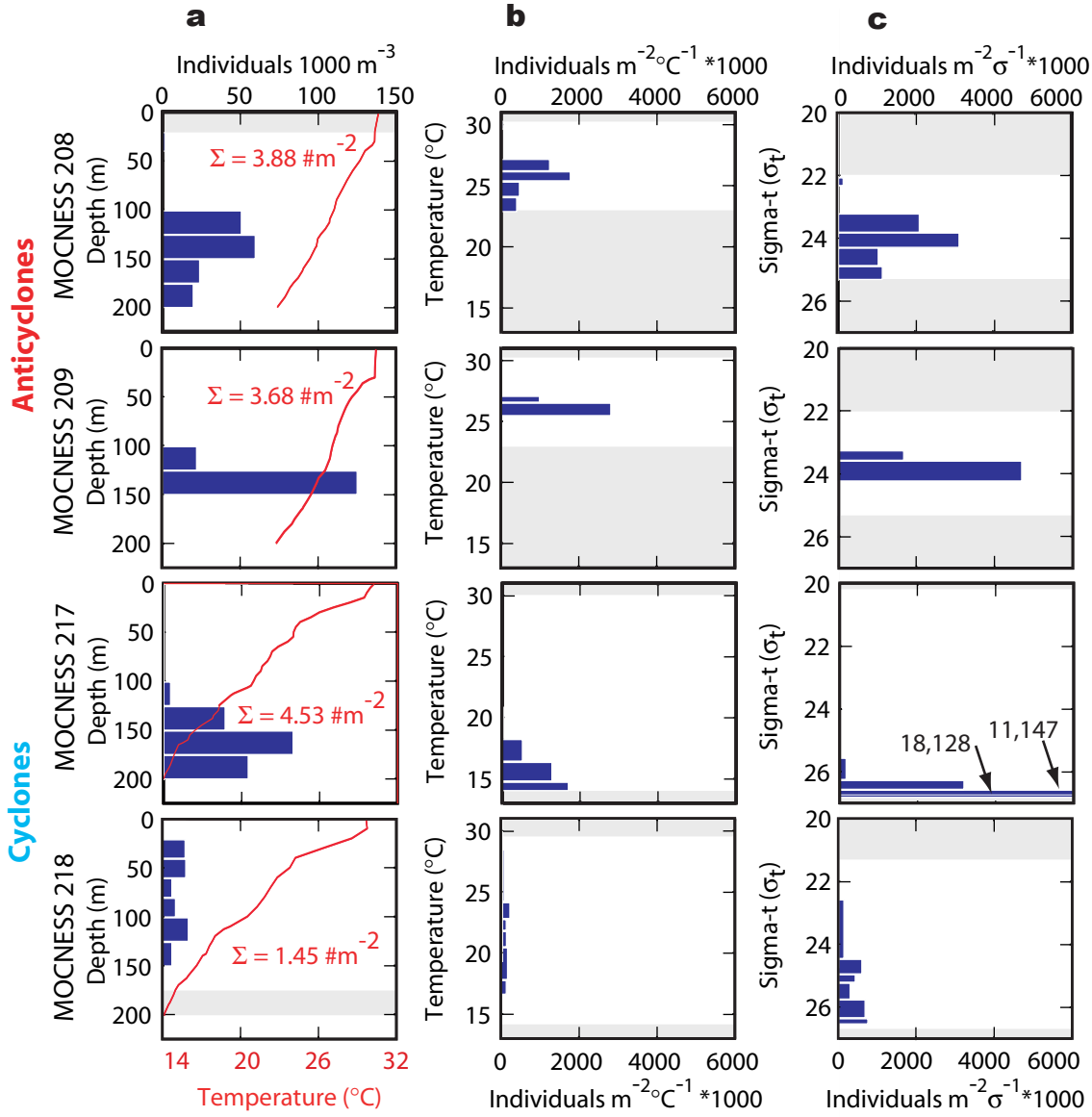

Fig. 21. *G. calida* property profiles. Column **a**: concentration (# 1000 m^{-3}) with temperature profile in red. Column **b**: temperature (# 1000 $m^{-2}°C^{-1}$). Each bar's width represents the temperature range found in the particular net. The height is the net's foraminifera abundance divided by the temperature range through the net, likewise, column **c**: density (# 1000 $m^{-2}\sigma^{-1}$). The resulting net areas integrate the same abundance shown in the corresponding net area of column **a**. Integrated tow abundances given in red. Gray shaded areas represent areas without data.

and *G. sacculifer;* and *G. siphonifera,* and *G. calida.* Two other species each have a unique pattern: *H. pelagica,* and *G. bulloides*. Each pattern may result from the sharing of a common ecologic niche and point to a specific controlling property.

O. universa and *G. menardii* share a similar factor 1 value, so is not surprising that their depth profiles are somewhat similar (**Figure 11; Figure 13 & Figure 14**). Also conspicuous is that both species are found minimally in the mixed layer. In the anticyclones, strong peaks with a bell-shaped distribution are found within the depth, temperature, and density profiles for both. The maximum concentrations occur at 80-100 m for *O. universa* and deeper for *G. menardii* at 100-125 m. In the anticyclones, the concentrations for both species peak sharply at ~27°C and 23 kg/m^3. Their cyclonic profiles, however, are dissimilar from each other and their anticyclonic counterparts. For *O. universa,* a maximum concentration forms shallower at 20-40 m corresponding to 24.2-28.6°C and 22.6-24.4 kg/m^3, but at 40-60 m a weak peak is seen for 24.2-22.8°C and 24.6-25.2 kg/m^3. This species is most abundant at 24-27°C for all tows. For *G. menardii,* the cyclonic tows do not show consistent behavior. Their profiles are characterized by a uniform concentration from 40 to 100 m, but with a maximum concentration found either at the top or bottom of this interval. In one tow MOC1-217, *G. menardii* has an unusual concentration spike between 100-125 m, ~20°C, and 25.5-26.24 kg/m^3. In the other cyclonic tow MOC1-218, the concentration peaks at the same depth as *O. universa*, 20-40 m, but is found most concentrated at ~22°C, and 24.9-25.1 kg/m^3. Although no property preference for *G. menardii* is apparent, the similarity in its profiles to *O. universa,* especially in the anticyclones, suggests a common factor that influences their depth distributions. Additionally among the tows, the absolute abundance for the two species appears within the same magnitude and is qualitatively comparable (**Table 4**). This pattern indicates that the nothing in either the anticyclonic or cyclonic environment particularly favors either of the species, but that the water properties are adequate.

The change in the species profile, however, indicates that they are tracking some preferred property. *O. universa,* and *G. menardii* are considered deeper water

opportunists (Hemleben et al., 1989; Bé, 1977), so they are expected to track the deep chlorophyll maximum (DCM) (Ravelo and Fairbanks, 1990). Considering the uncertainty of the chlorophyll profiles at the MOCNESS stations and the inherent imprecision in the calculated median depth values, the fact that seven of the eight samples are within one net interval of the estimated chlorophyll maximum identifies chlorophyll as the property these two species track (**Figure 5 & Table 7**). Even without precise direct chlorophyll measurements, a qualitative explanation correlates these species with the peak chlorophyll concentrations.

Another species *H. pelagica* has its own unique profiles and factors for a common species with only two rare species plotting nearby: *G. tenellus* and *G. truncatulinoides* (**Figure 11**). The abundance of *H. pelagica* does not correlate with either eddy class nor does it not consistently concentrate at any hydrographic property across all the tows (**Figure 15**). The two largest abundances of *H. pelagica* are in one anticyclonic tow MOC1-208 and a cyclonic tow MOC1-218 with the other tows containing about half to a quarter of these abundances. In the anticyclones, however, it does peak at 125-150 m and ~26°C. In the cyclones, the peaks only correspond to the density anomalies at 26.5 – 26.8 kg/m^3. The narrow concentration bands probably indicate other environmental controls on its distribution that track these examined properties. Isolating the specific properties that *H. pelagica* prefers is difficult because of the inconsistent abundances and profiles among the tows.

H. pelagica is described as "predominately, if not exclusively, carnivorous" like *G. menardii* and *O. universa* (Hemleben et al 1989), and so should track the DCM like *O. universa* and *G. menardii*. In the two tows where *H. pelagica* appears at comparable abundances (greater than 4#m^{-2}), its concentrations appear relatively even through a 150 m interval, but weakly peaking at the expected DCM (**Figure 14**). The fragile test of this particular foraminifera may have resulted in lost individuals during collection, preservation, and sampling (Thunell and Honjo, 1981); hence obscuring its relationship with the DCM.

Three other species share another pattern and similar factor 1 and 2 values: pink and white *G. ruber,* and *G. sacculifer*. Their factor 1 values are within 3% of each other and their factor 2 values within 6% (**Figure 11**). These three species have their highest concentrations at the surface, but do not seem to correlate to temperature or density across all the tows (**Figures 16, 17, & 18**). For the white *G. ruber*, the largest abundances are in the cyclonic tows at 1.3% with the cyclones totaling only three individuals. Such small abundances bar any strong generalizations for white *G. ruber* distributions across both regimes. Likewise, *G. sacculifer* does not seem to have any temperature, or density preference across all the tows. However, the shape of its depth profile in all the tows seems to indicate a surface preference. The maximum concentration occurs between 0-40 m for three tows. In the fourth tow, the anticyclonic MOC1-208, the surface net is missing and the difference among its other nets is small. The highest concentration is at 80-100 m, but the difference between the surface concentration of 20 and the maximum of 27 per 1000 m^3 may not be significant. In the tows where the three species occur in an abundance above a few percent, a preference for the upper 60 m of the water column is apparent.

G. ruber and *G. sacculifer* are highly dependent on their algae symbionts to survive and so should have preference for the upper water column (<50 m) where light levels are sufficient for their symbionts (Watkins et al., 1996; Faul et al., 2000). In both anticyclonic and cyclonic environments, the surface light conditions are similar, but the thicker mixed layer in the anticyclones constantly mixes the species further down into the water column and into less light. The base of the mixed layer in the anticyclones has about 20% of surface incident radiation, whereas in the cyclones about three times more (66%) is available (**Figure 6**). The thinner mixed layer in the cyclones makes it easier for these species to stay closer to higher light levels at the surface. With less energy expended to stay at high light levels and the resulting enhanced nutrition, these species flourish in the cyclones. The difference in temperature and density between the two environments does not directly enrich the abundance of the species in the cyclones, but

the resulting deeper anticyclonic mixed layer does hamper these species from prospering.

G. bulloides has its own pattern among the tows, but has factor 1 and 2 values that are similar to six other species (**Figure 11**). Unlike any other species though, it has a bimodal distribution with peaks at 20-40 m, 22.8-24.5°C, 24.4-24.9 kg/m^3 and 125-150 m, 16.4-18.3°C, and 26.3-26.7 kg/m^3. For each peak, the peak values do not correspond to the same interval in the water column (**Figure 19**). The species also is not present in one anticyclonic tow (MOC1-209) and at less than 1% in the other, so correlating its abundance to temperature is only valid for the cyclones. *G. bulloides* is a sub-polar species (Bé and Tolderlund, 1971), so the warmer temperatures of the anticyclones may exclude its presence even where other conditions are ideal. In the cyclones, the cooler temperatures in conjunction with another property allow it to prosper.

Why does *G. bulloides* become the most abundant in the cyclones, whereas it is nearly absent in the anticyclones (0.55% of the total anticyclone abundance)? Its diet is unsupported by any symbionts, and so it is estimated to have one of the highest prey demands to survive (Ortiz et al., 1995). They must thrive when cooler temperatures occur in conjunction with available phytoplankton. In tropical and subtropical provinces, this subpolar species is characteristic of upwelling and convergence zones where it can thrive in the colder surface waters and where the higher productivity and prey concentrations result from the upwelled nutrients (Schiebel et al., 1997 and ref. therein). These conditions correspond to the cyclones of this study where cooler temperatures (less than 26°C) in the upper 75 m of the water column and sufficient phytoplankton concentrations (a peak at about 80 m) exist to allow *G. bulloides* to thrive. In these situations, *G. bulloides* corresponds to a surface species (~0-50 m) rather than a subsurface species (~75-225 m).

Finally, *G. siphonifera* and *G. calida* share similar depth profiles and factor 2 values with inverted factor 1 values (**Figure 11**). In addition, neither has a depth, temperature, or density profile that is consistent across all four tows (**Figure 20&21**).

Across three tows, they show a preference for deeper waters, peaking between 125-175 m. The temperature plots for these three tows shows the species concentrated in a narrow interval: ~25°C for the anticyclonic tows, and ~15°C for the cyclonic tow. The fourth, a cyclonic tow MOC1-218, is inconsistent with these previous tows. For both species, it has two peaks shallower than the previous tows. Here, *G. siphonifera* abundances peak at 100-125 m with another smaller peak at 40-60 m. *G. calida* peaks at 100-125 m with another smaller peak through 20-60 m. Potentially, the missing last net of cyclonic tow MOC1-218 (175-200 m) could explain the inconsistent behavior, but this possibility seems unlikely. The last two nets of MOC1-218 (125-175 m) have minimal abundances of *G. siphonifera* and *G. calida*. The net from 150-175 m has neither species. The next net 125-150 m has a minimal abundance of *G. siphonifera* with less than a third of the peak abundance and the lowest abundance of *G. calida.* The high abundances in the earlier nets and minimal abundances collected in the bottom two nets makes the likelihood of significant contributions of *G. calida* and *G. siphonifera* in the missing last net unlikely. Generally, both are morphologically similar (Parker, 1962), which suggests an adaptation to the same ecologic niche that in this study points to a preference for depths of 125-175 m. However, the inconsistent behavior represented in MOC1-218 makes this a tentative conclusion.

Among all the species, a shift in the dominant species and depth of maximum abundance found between the two environmental regimes is hypothesized to directly follow one of three hydrographic properties: depth (or a depth dependent property), temperature, or density. The profiles of each species, however, are inconsistent against the examined hydrographic properties (**Table 10**). Only two species had a maximum concentration consistently correlate across all the tows: pink *G. ruber,* and *G. sacculifer* for depth (**Table 10**). These two species along with white *G. ruber*, *G. bulloides*, *G. conglobatus* and *G. crassiformis* are the species that had a high factor 1 value (**Figure 11**). All these species are at least an order of magnitude greater in the cyclones than in the anticyclones. All the positive factor 1 species are also found in specific depth ranges, whereas the negative factor 1 species are found more dispersed through the

Table 10. Summary of high species concentrations occurring at specific properties. "Both" indicates that the same value is found among all the tows. Otherwise "Anticyclone" or "Cyclone (Cycl)" indicates a value consistent only in that environment.

Species	Depth	Temperature	Density	Chl a
O. universa	Cycl/Anticyclone	Cycl / Anticyclone	Cycl / Anticyclone	Anticyclone
G. menardii	Anticyclone	Anticyclone	Anticyclone	Anticyclone
G. ruber (pink)	Both			
G. ruber (white)	Cyclonic			
G. sacculifer	Both			
H. pelagica	Anticyclone	Anticyclone	Cyclone	
G. bulloides				
G. siphonifera	Anticyclone	Anticyclone		
G. calida	Anticyclone	Anticyclone		

upper water column. *H. pelagica* and *G. tenellus*, both high factor 2 species, however, have similar profiles among the tows, but do not correspond to either eddy type or any of the examined hydrologic properties. The remaining high Factor 2 species, *G. truncatulinoides* is simply found at the bottom of the tows (data not shown). *G. menardii* is unique in that it has the lowest factor 2 value, but what this factor correlates to is inexplicable (**Figure 11**).

In just the anticyclones, five species concentrate at a particular depth and temperature: *O. universa, G. menardii, H. pelagica, G. siphonifera,* and *G. calida*. Two of these species also concentrate at a density: *O. universa,* and *G. menardii* (**Table 10**). In the cyclones, *O. universa* is found concentrated at specific values for all three of the examined properties, whereas white *G. ruber* at a depth, and *H. pelagica* at a density (**Table 10**).

The change in the dominant species and depth between the two regimes is due to changes in the depth dependent properties. The species dominating the anticyclonic tows have a general preference for deeper depths (greater than 50 m): *O. universa, G. menardii*, *G. siphonifera,* and *G. calida,* (Bé, 1977). All these species can have symbionts except *G. calida*, nevertheless these species depend more on prey capture than their symbionts to survive (Bé, 1977; Hemleben et al., 1989). The peak abundances for these species are expected to coincide with the deep chlorophyll maximum in typical oligotrophic environments (Fairbanks and Wiebe, 1980; Fairbanks et al., 1982). The interval above and below the presumed chlorophyll maximum accounts for about 60% of the anticyclonic abundances (**Figure 5**&**Table 7**). The cyclonic dominating species, however, prefer surface waters (less than 50 m) e.g., pink *G. ruber*, *G. sacculifer* (Watkins et al., 1996), and *G. bulloides* (Faul et al., 2000). These three species abundances peak shallower in the cyclones with 50% and 70% of the population encapsulated between 0-60 m. Although, the species dominating the anticyclones are deeper-dwelling species and are probably following the deep chlorophyll maximum, the cyclonic species do not correspond to the deep chlorophyll maximum. The cyclonic upwelled waters keep their dominant species within an

environment in which they can flourish: high light levels for *G. ruber* and *G. sacculifer;* cooler temperatures for *G. bulloides*.

In the Panama Basin, other MOCNESS research found white *G. ruber, G. sacculifer,* and *G. bulloides* co-occurring (Fairbanks et al., 1982). Pink *G. ruber* was not described. In the study, the mixed layer was about 25 m deep with a temperature of 26ºC, and a chlorophyll peak of ~0.45 $mg \cdot m^{-3}$at its base, which according to the present study are ideal conditions for *G. bulloides.* The species was found in three of their four tows and at abundances of the same magnitude as the Gulf samples. White *G. ruber* was found at two orders higher and *G. sacculifer* (without sac) one order higher. As with the present study, all three species were found at the highest concentrations in the surface net (upper 20 m). Another species *H. pelagica* occurred in each tow at the same order of magnitude as *G. sacculifer* (without sac). Both species had their peak concentrations in the upper 50 m with *H. pelagica* peaking at about 35 m where chlorophyll concentrations are nearly peak values (~0.4 $mg \cdot m^{-3}$). In the Gulf of Mexico, *H. pelagica* also follows chlorophyll concentrations, but its abundances were an order of magnitude lower, and no similarity to *G. sacculifer* was found. The peak concentrations of *O. universa* and *G. menardii* also coincided with the largest chlorophyll concentrations as was the case in the Gulf. Unlike the present study, in the Panama Basin these species share no common pattern in their depth profiles. Finally, *G. siphonifera* (synonym *G. aequilateralis),* and *G. calida* were found in the Panama Basin at abundances at least two orders of magnitude greater than those found in the Gulf of Mexico. Symbiont-laden variants of *G. siphonifera* occurred with at least twice the abundance of *G. calida. G. siphonifera* (both symbiont laden and symbiont barren) and *G. calida* consistently were found in the upper 100 m, but *G. calida* was absent from the surface to 50 m. The concentration profiles in the Gulf suggest that both *G. siphonifera* and *G. calida* have a preference for deeper waters (125-175 m). The Panama profiles correspond to this preference for *G. calida* in the Gulf*,* but contradict for *G. siphonifera*. A comparison to the Gulf samples is not valid, because the abundances of *G. siphonifera* were two orders of magnitude higher in the Panama Basin and a distinction was made between between

symbiont barren and laden individuals. The profiles of the other eight common species, however, can be explained by the results of the current study.

Another study described the foraminifera population changes from Atlantic Slope waters through a cold core ring to Sargasso Sea water in the Western North Atlantic (Fairbanks et al., 1980). The rings contrast with the Gulf eddies in that the rings are composed of distinct water masses from the surrounding waters of the Sargasso Sea, whereas both eddy types are composed of the same water masses shifted up or down within the water column. Investigators found thirteen species that included all the common species found in the Gulf except *G. calida.* The profiles and abundances of the species found in both environments can be explained by the results of the current study. For example, pink *G. ruber, G. sacculifer,* and *G. bulloides* all had their highest concentrations in the upper 50 m of Slope waters where the greatest stratification occurs. In the rings, more of the pink *G. ruber* and *G. sacculifer* population were dispersed deeper, but as described in the current study, this mixing results in a smaller total abundance. The abundance of *G. ruber* drops to a tenth and *G. sacculifer* to half the Slope abundances. Also as a result of this mixing, no *G. bulloides* was found in the ring. Trace concentrations of pink *G. ruber, G. sacculifer,* and *G. bulloides* were found in the warmer Sargasso Sea water. The abundance of *O. universa* dropped in a similar fashion from the high Slope populations to the minimal Sargasso Sea abundances. *O. universa* had its highest concentrations in the upper 75 m of Slope waters with a maximum at the surface 0-25 m. However in the cold core ring, the highest concentrations shift to a deeper depth between 25-150 m. Relative to their source Slope waters, cold core rings are warmer since they warm as they decay in the Sargasso Sea (Fairbanks et al, 1980). This profile change also occurs in the Gulf from a shallower peak in the colder cyclones to a deeper peak in the warmer anticyclones. As described in the current study, temperature does not exclusively control the distribution of *O. universa* through the water column. This omnivorous species is probably following the deep chlorophyll maximum, and the deeper mixed layers of the warmer environments push the DCM and thus its population deeper. According to our research, *G. menardii* abundances should

follow *O. universa* abundances and profiles. However in the Atlantic, *G. menardii* were a half to a tenth of the Gulf abundances. As their population decreased through warmer waters, the remaining individuals were found inexplicably shallower. The *H. pelagica* population also follows a similar pattern. In terms of the Gulf of Mexico results, the distributions of *G. menardii* and *H. pelagica* are inexplicable. Finally, where their *G. siphonifera* abundances in the warmer Sargasso Sea drop by an order of magnitude to comparable Gulf values, the species appears to prefer deeper waters as in the Gulf. Only where *G. siphonifera* abundances are lower than 10.0 $\#m^{-2}$ does this preference for deeper waters exist. Otherwise, where it occurs at greater abundances, this preference disappears. For example in the Slope waters, where its abundance was an order of magnitude higher was it found concentrated in the surface/mixed layer. *G. siphonifera* may have had algal symbionts, so the shallower mixed layer facilitated its access to more light and sufficient nutrients. The research in the Gulf of Mexico shows further mechanisms to explain the depth distribution of foraminifera than what earlier studies described (e.g., Bé, 1977; Fairbanks et al, 1980; Fairbanks et al, 1982; Hemleben et al, 1989).

The above differences between the anticyclonic and cyclonic regimes are not due to timing of the sampling. Given that it takes a foraminfera (*G. sacculifer)* two to three days to grow from 100 to 200 μm (Bijma and Hemleben, 1994), then it is possible that our sampling missed a juvenile population in the anticyclones that were mature when the cyclones were later sampled. However since juveniles smaller than 150 μm are collected across both regimes, it is reasonable to expect the same percentage of the juvenile population to be collected in either regime. Because at least order of magnitude change for the three species is found in the cyclones, but no corresponding juvenile population in the anticyclones, the above scenario is unlikely. In addition, Bijma et al (1990b) found the abundance of *G. sacculifer* and *G. ruber* reaches a maximum about nine days before a full moon. Here, the foraminifera are collected starting twelve days before a full moon or three days after a new moon (**Figure 22)**. During the five days of sampling, the anticyclonic samples were collected before the expected maximum and

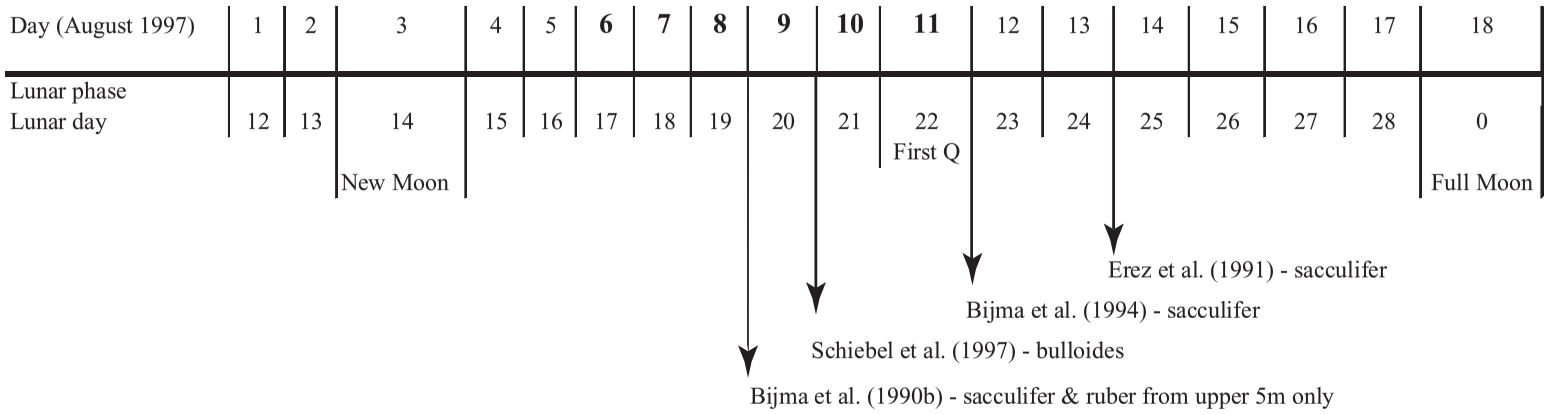

Fig. 22. Comparison of sample collection and lunar cycle dates. Dates of other researcher's maximum abundances are indicated. Our collection dates are bolded.

had the least number of individuals; whereas the cyclonic samples were collected after the expected maximum and had the most number of individuals (Bijma et al., 1990b; Erez et al., 1991; Schiebel et al., 1997). Our collection dates seem to rule out the foraminifer's reproductive cycle as a cause for the population differences seen in the different regimes. The 50% greater zooplankton biomass in the cyclones also strengthens our contention that the foraminifera differences are not the result of sampling during a particular foraminfera reproductive phase, but represent accurate populations. Likewise, our samples were collected at nearly the same time across the cruise dates, which excludes finding variations due to any diel migration of the foraminifera. Even if planktonic foraminifera followed the pattern of many other zooplankton, feeding at the surface at night and sinking to lower depths during the day (e.g., pteropods, Wormuth, 1981), the samples were collected at nearly the same times (**Table 1**). Typically, these diel migrations are initiated before sunset and sunrise. Our tows occurred several hours after sunset or before sunrise. Also, the anticyclonic MOC1-209 and cyclonic MOC1-217 tow were collected at the about the same time and contained vastly different concentrations and abundances of foraminifera species, indicating that their location and not time was the critical variable controlling the foraminiferal abundance. *G. bulloides* concentrations, for instance, varied across three orders of magnitude between these tows. All the samples were collected across a five hour interval which was not across a potential diel migration (**Table 1**). The differences seen between the anticyclonic and cyclonic regimes are not due to our sampling dates or times.

Nevertheless, an unusual circumstance is the abundant co-occurrence of a tropical, sub-tropical, and sub-polar species: *G. sacculifer, G. ruber,* and *G. bulloides.* Likewise, two of these species are adapted to oligotrophic conditions and another to more productive waters. The oligotrophic species *G. ruber,* and *G. sacculifer* are dependent on prey capture to survive, but can survive and reproduce with an occasional prey capture every one to four days (Bé, 1982). Watkins et al (1996) concluded these species are best adapted to oligotrophic waters because the abundance of these species

decreased as primary productivity increased. In more productive waters, the more opportunistic foraminifera and zooplankton can out compete these *Globigerinoides* species. The dietary advantage of their symbionts becomes a liability in the possibly light-limited environments of more productive waters (Watkins et al., 1996). This pattern is not found here with pink *G. ruber* and *G. sacculifer* summing to higher population than the completely opportunistic *G. bulloides.*

In the cyclones, the most abundant species is the sub-polar *G. bulloides* and the next most abundant species is the warmer sub-tropical pink *G. ruber*. It is not unusual to find these species together in upwelling areas, but not at the integrated abundances of the same magnitude as found in this study (Fairbanks et al., 1980; Fairbanks et al., 1982; Oberhänsli et al., 1992; Schiebel et al., 2001; Peeters et al., 2002). Atypical also is the similar abundance of *G. sacculifer* and *G. ruber*. Usually, one species dominates the other in abundance because each species is adapted to a particular ecologic niche (Reiss et al., 1999). In this study, the tropical *G. sacculifer* occurs with at least half the abundance of *G. ruber*, if not the same.

Neither physical nor chemical characteristics of the cyclones alone explain these abundant concurrences. A large anticyclonic *G. bulloides, G. ruber,* and *G. sacculifer* population would have to exist between 200 m to about 350 m if advection is responsible for the dramatic increase in the cyclonic abundances. This scenario seems unlikely because this depth interval is outside the range of these species (Emiliani, 1954; Bé, 1977; Fairbanks et al., 1982). Also unlike the Atlantic rings, the population structure changes do not result from differing water masses and do not represent a biogeographic shift because the cyclonic and anticyclones features are formed from the same water masses. Finally, the cyclonic and anticyclonic eddies are on the order of months old, so it is unlikely that the species represent transient populations changing from one environmental regime to another, but are truly coexisting populations. Initially, Bé and Tolderlund, (1971) concluded that the biogeographic distinction between *G. sacculifer* and *G. ruber* are salinity controlled since *G. ruber* is found at oceanic salinity extremes where *G. sacculifer* is absent. Bijma et al (1990a) showed the

existence or dominance of either species is probably not salinity controlled, but is the result of to an adaptive advantage that one species may have over the other (e.g., nutrient exploitation). Ufkes et al (1998) attributed the co-appearance of warm, oligotrophic *G. ruber* with the cold, higher productivity water *G. bulloides* to frontal mixing of warm Congo River water with coastal upwelled waters. This mechanism cannot explain the concurrence of these species in the Gulf of Mexico. The results of this study, showing the concurrence of *G. bulloides, G. sacculifer,* and *G. ruber* at similar concentrations, is inexplicable in terms of physical or chemical properties, but probably is due to an underlying biologic factor.

The plankton composition, I believe, is responsible for the species abundances of *G. bulloides, G. sacculifer,* and pink *G. ruber* co-occurring at comparable high abundances. *G. bulloides* lacking any symbionts depends on prey capture to survive, but may be primarily herbivorous (Schiebel et al., 1997). *G. ruber* is also a weak zooplankton predator, but *G. sacculifer* is an aggressive *Globigerinoides* species (Fenton et al., 2000 and ref. therein). *G. sacculifer* should out compete *G. ruber* in environments dominated by higher zooplankton organisms such as copepods (Hemleben et al 1989; Bijma et al., 1990a; Fenton et al., 2000). An environment that favors the herbivorous foraminfera will rank the abundance of *G. bulloides*, *G. ruber*, and then *G. sacculifer* as in this study. Also, the poor abundances of carnivorous *H. pelagica* support the supposition that the plankton was primarily phytoplanktic.

However, even if preferred zooplankton prey are abundant, *G. ruber* will out compete *G. sacculifer* if nutrient concentrations are high (Bijma et al., 1990a; Bijma and Hemleben, 1994). In the Gulf, the nitrate levels are below the detection limit in the upper 60 m where these species peak, so nutrient concentrations alone are irrelevant (Biggs 1992). Regardless, where nutrients are high and phytoplankton has yet to bloom, *G.* ruber will not thrive (Peeters et al., 2002). In this study however, nutrients are undetectable at the surface and phytoplankton are sufficient for all these species.

The herbivorous species dominance also cannot be attributed to differences in the timing or location of reproduction (Bijma et al., 1990b; Schiebel et al., 1997). The

herbivorous *G. bulloides*, and the carnivorous *G. sacculifer* reproduce on a lunar cycle and are the most and least abundant, respectively of the three species. The herbivorous *G. ruber*, which reproduces on a semi-lunar cycle (2 weeks), ranks between them. Likewise, the deeper reproductive depth of *G. bulloides* and *G. sacculifer* do not appear to place them at a disadvantage to the shallower reproducing *G. ruber* (Auras-Schudnagies et al., 1989; Bijma and Hemleben, 1994; Schiebel et al., 1997; Reiss et al., 1999; Fenton et al., 2000 and ref. therein). The dominance of the herbivorous species over the more carnivorous species may indicate a planktonic composition that is primarily phytoplanktonic and sparse in higher zooplankton species.

In another study, Peterson et al (1991) used the dominance of *G. bulloides* or pink *G. ruber* as an indicator of the local upwelling or non-upwelling season in the Cariaco Basin. Here, the authors didn't speculate as to what the disproportionate spikes in the pink *G. ruber* abundances meant in their cores. One pink *G. ruber* peak corresponds to a drop of the *G. bulloides* from about half the abundance to about 20%. The other *G. ruber* peak corresponds to an intermittent peak of G. *bulloides* to nearly its former abundance. The results of this study imply that when both these species occurred at high abundances, they may have an ecology similar to that of the Gulf cyclones – an upwelling that brought nutrients into the photic zone and favored a more herbivorous foraminifera.

When interpreting downcore abundances of the above species, investigators should consider several particular characteristics of these foraminfera. First, pink *G. ruber* is extinct in the Pacific, so research qualitatively describing the ecology of its white variant may not apply in describing the pink variety (e.g., Fairbanks et al 1980, 1982; Ortiz et al., 1995; Watkins et al., 1996). Other studies may have neglected making the distinction between pink and white variants (e.g., Oberhänsli et al., 1992; Boltovskoy et al., 1996). Oberhänsli et al (1992) claim that their processing fades the color out of their *G. ruber* samples. In contrast, various authors note that the white variety occurs throughout the year whereas the pink *G. ruber* only occurs in the summer (e.g., around Bermuda (Bijma et al., 1990a) or the Cariaco Basin (Lin et al., 1997)). The

pink variety behaves differently from the white variety in typical oceanic conditions and this behavior probably extends to upwelling/convergence regimes (Bé and Tolderlund, 1971; Peterson et al., 1991; Ufkes et al., 1998). The results of this study concur with these conclusions and investigators must distinguish between pink and white varieties when interpreting *G. ruber* shell data. Secondly, *G. ruber* reproduces on a semi-lunar cycle whereas *G. sacculifer* and *G. bulloides* reproduce on a lunar cycle, so the later two must be twice as prolific in the water column to maintain similar abundances on the seafloor (Bijma et al., 1990b). In the cyclones, *G. sacculifer* and *G. bulloides* are found in least comparable if not greater abundances and so are more prolific. Nevertheless, the semi-lunar reproductive cycle of *G. ruber* results in this species potentially recording or averaging sea surface conditions at twice the temporal resolution of the other two species. Finally, abundances of *G. bulloides* can correspond to upwelled specimens, so sites where high sediment concentrations of *G. bulloides* can indicate high productivity and upwelling (Faul et al., 2000).

G. sacculifer is a species that is commonly applied to reconstruct sea surface conditions. The depth profiles and abundances found in this study support its use in these projects. More than 85% of the *G. sacculifer* is found above 40 m centered at about 28 ±2.5ºC. This results in up to a ±0.5 variance in the isotope values (**Figure 23**) (Erez and Luz, 1983). However, 75% of the population exists within a smaller temperature range between 30-28ºC and results in an isotope variance of ±0.3. In our net sampling, about 37% of the *G. sacculifer* was found explicitly in this interval. Another 40% of the population was sampled through this temperature interval but the sampling also continued through to 24ºC. In the other samples, however, only 3% of the population was found explicitly from 28-24ºC. The majority of the individuals found in the one interval from 30-24ºC were in all likelihood contained within the smaller temperature range of 30-28ºC, but our sampling scheme obscures this resolution. *G. sacculifer* is found and so grows in the temperature at the surface/mixed layer. Our results show that about 75% of the *G. sacculifer* found downcore represents the surface mixed layer. The remaining quarter may reflect colder conditions within the photic zone

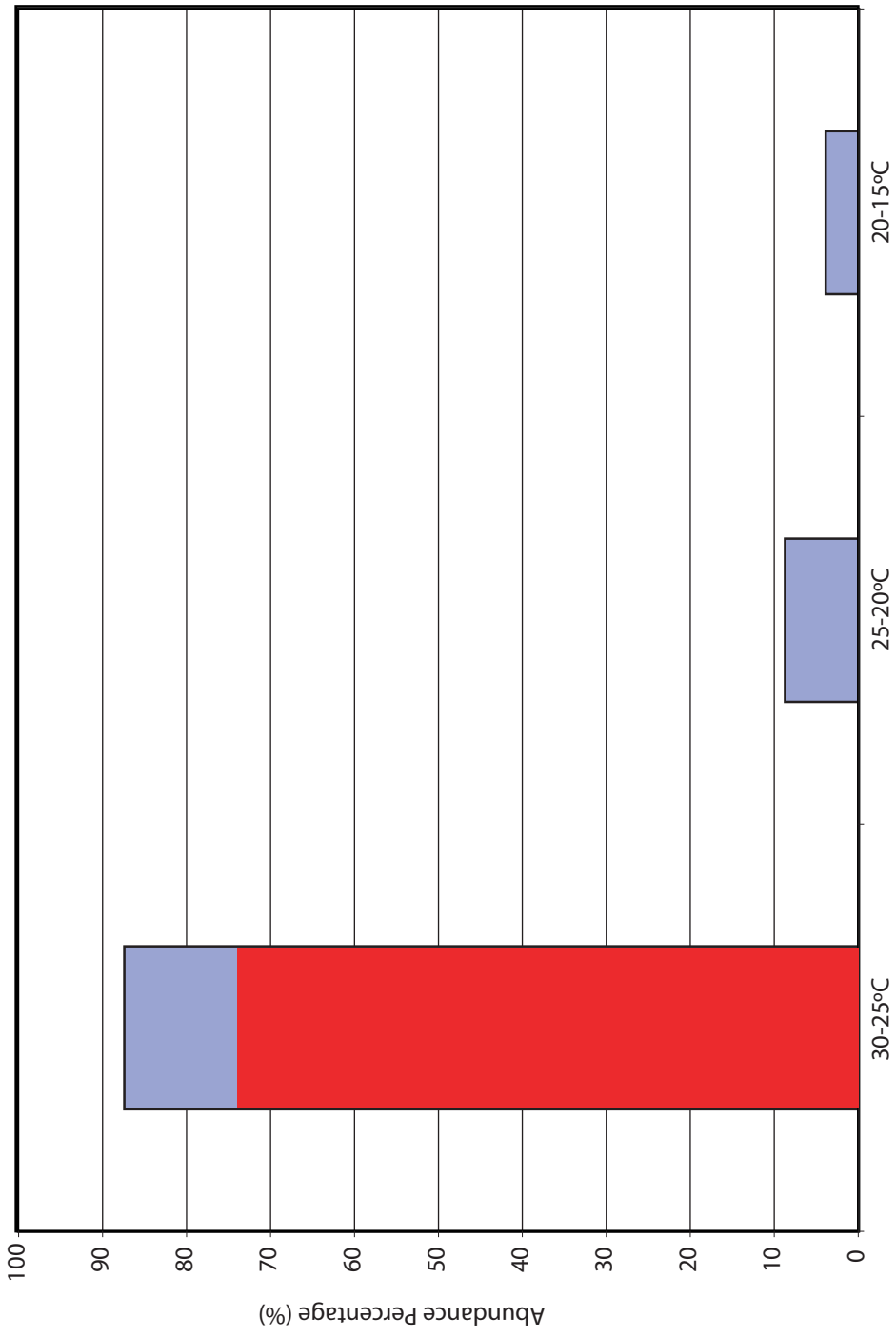

Fig. 23. Temperatures coresponding to percentage of *G.sacculifer* abundance. Red area represents abundance probably found between 28-30°C.

or possibly species that are no longer growing and descending out the mixed layer (Fairbanks et al., 1982).

Also in the Gulf, the drastic increase of pink *G. ruber, G. sacculifer,* and *G. bulloides* from the anticyclones to cyclones may bias the interpretation of downcore values towards the cyclonic conditions. The potential two orders of magnitude increase of these foraminifera in the cyclones can overwhelm the signal from their counterparts settling from typical Gulf waters or anticyclones. This scenario is highly possible since up to three anticyclones may exist west of 90ºW and that one or more cyclonic areas are associated with them (Biggs, 1992 and ref therein). Synder (1978) found *G. bulloides* in the surface sediments of our study area range from 0-10% in relative abundance, whereas *G. ruber* and *G. sacculifer* range from 20-25 % and 4-8%, respectively. The cyclonic proportions of these three species influxing about once to twice a month from passing cyclones can create the appropriate ratio of *G. bulloides* and *G. sacculifer* abundances, but would underestimates the *G. ruber* abundance by about 20-50%. (This estimate assumes that anticyclonic waters are close to typical Gulf waters, and that *G. ruber* the influx occurs at twice the frequency of the other species.) The foraminifera found in sediments could readily represent the cyclonic seawater conditions rather than the typical Gulf waters or anticyclones. Before using the popularly applied *G. ruber* or G. *sacculifer* data to paleoclimatic reconstructions, investigators should check the species assemblage to see if cyclonic species (e.g., *G. bulloides*) are also present. Otherwise, the foraminfera they pick from their sediment samples may represent atypical cyclonic conditions.

IV. SUMMARY AND CONCLUSIONS

All the tows are composed of the same water masses, but the masses are upwelled in the cyclonic tows and depressed in the anticyclones resulting in a shift of the measured profiles (**Figure 2-5**). As a response to some of the changes in these environmental parameters, a corresponding shift in the foraminfera abundances and depth profiles occurs (**Figure 9&10**). The absolute abundance of foraminifera is enriched in the cyclonic environments with the three species tripling the foraminferal abundance: pink *G. ruber, G. sacculifer*, and *G. bulloides*. These same species comprise less than 15% of the abundance in the anticyclonic tows. Four species that do compose 15-25% of the cyclonic tows, comprise 90% of the abundance in the anticyclonic tows: *O. universa, G. menardii, G. siphonifera,* and *G. calida* (**Table 4**). The species shift occurs as each environment has some water property that the dominating species can better exploit (Ortiz et al., 1995).

Foraminifera populations exploit these properties by concentrating at its location in the water column to feed (reflected by available prey, light, or available nutrients) or to avoid being fed upon. They are adapted to track these specific temperatures or densities that have optimal feeding or concealing potential. This behavior means that they track specific hydrographic features such as the chlorophyll maximum, and the thermocline depth as found in this study, and so their calcification depth and temperature are not necessarily consistent (Faul et al., 2000; Ravelo and Fairbanks, 1992). Like the present study, *G. ruber* and *G. sacculifer* were found to thrive where light levels are the highest, independent of nutrient and chlorophyll levels (Faul et al., 2000). Seven other species, however, are inconsistently correlated across all the tows with any one of the examined water properties. For *G. bulloides*, where both the temperature is below 26ºC and food still sufficient (chlorophyll), the sub-polar species is found to dominant the foraminiferal abundances of the sub-tropical environment of the Gulf of Mexico. Three

other species are not consistently tracking any single hydrographic property, but probably chlorophyll: *O. universa, G. menardii,* and *H. pelagica.* Two other species *G. siphonifera* and *G. calida* are found to prefer depths of 125-175 m, but this characterization does hold where the abundances of these species are higher (e.g., Fairbanks et al, 1980; Fairbanks et al, 1982). All the common foraminifera species concentrate in narrow bands indicating that hydrographic properties do influence their distributions, but they were not found to follow any specific values.

Formainifera, however, are adapted to specific habitats defined by specific ranges of temperature, salinity, turbidity, etc. that define the biogeographic provinces in which they can survive. Within these provinces, these physio-chemical factors do not directly control their abundance (Oberhänsli et al., 1992; Ortiz et al., 1995; Watkins et al., 1996). Their abundances within their depth habitats probably reflect where they are fulfilling their dietary requirements, hence able to quickly reach adulthood and reproduce (Ravelo and Fairbanks, 1992). Thus, the abundance of foraminifera at an upwelled water mass does not reflect simple advective accumulation, but an exploitation of the resultant biologic productivity to meet their dietary requirements (Watkins et al., 1996).

Ideal conditions for specific foraminifera can cause abundance changes of two orders (e.g., *G. bulloides).* A few instances of these ideal conditions can bias data away from typically poor conditions and abundances. Investigators removing a single species from a sediment assemblage for chemical analysis should first examine the entire the assemblage to determine if it accurately reflects a hydrographic environment they wish to reconstruct (e.g., a truly pelagic environment versus an upwelling region such as eddies or rings). When interpreting downcore abundances, investigators must consider how the above described physical, chemical, and biologic factors influence foraminfera distributions through the water column.

REFERENCES

Auras-Schudnagies A., Kroon D., Gassen G., Hemleben C., and Van Hinte J.E. (1989) Distributional pattern of planktonic foraminfers and pterpods in surface waters and top core sediments of the Red Sea, and adjacent areas controlled by the monsoonal regime and other ecological factors. *Deep-Sea Res.* **36,** 1515-1533.

Andreasen D.J., Ravelo A.C. (1997) Tropical Pacific Ocean thermocline depth reconstruction for the last glacial maximum. *Paleoceanography* **12,** 395-413.

Bé A.W.H. (1977) An ecological, zoogeographic and taxonomnic review of recent planktonic foraminifera. In *Oceanic Micropaleontology Vol 1*, (ed. A.T.S. Ramsay), pp. 1-100. Academic Press.

Bé A.W.H. (1982) Biology of planktonic foraminifera. In: *Foraminifera: Notes for a short course.* (ed. T.W. Broadhead), pp 51-92. The University of Tennessse, Knoxville.

Bé A.W.H., and D.S. Tolderlund (1971) Distribution and ecology of living planktonic foraminifera in surface waters of the Atlantic and Indian Oceans. In *The Micropaleontology of the Oceans* (ed. B.M. Funnell and W.R. Riedel), pp104-149. Cambridge University Press.

Biggs D.C. (1992) Nutrients, plankton and productivity in a warm-core ring in the Western Gulf of Mexico. *J. of Geophys. Res.* ***97,*** 2143-2154.

Bijma J., and Hemleben C. (1994) Population dynamics of the planktic foraminifer *Globigerinoides sacculifer* (Brady) from the central Red Sea. *Deep-Sea Res. I* **41,** 485-510.

Bijma J., Faber jr. W.W., and Hemleben C. (1990a) Temperature and salinity limits for growth and survival of some planktonic foraminifers in laboratory cultures. *J. Foraminiferal Res.* **20,** 95-116.

Bijma J., Erez J., and Hemleben C. (1990b) Lunar and semi-lunar reproductive cycles of some planktonic foraminifers. *J. Foraminiferal Res.* **20,** 117-127.

Billups K., and D.P. Schrag (2000) Surface ocean density gradients during the Last Glacial Maximum. *Paleoceanography*. **15,** 110-123.

Boltovskoy E., Boltovskoy D., Brandini F. (2000) Planktonic Foraminfera from south-western Atlantic epipelagic waters: abundance, distribution and year-to-year variations. *J. Mar. Biol. Ass. U.K.* **79,** 203-213.

Boyle E.A. (1981) Cadmium, zinc, copper, and barium in foraminifera tests. *Ear. Plan. Sci. Let.* **53,** 11-35.

Chen M.T., and Prell W.L. (1998) Faunal distribution patterns of planktonic foraminifers in surface sediments of the low-latitude Pacific. *Palaegeogr., Palaeoclimatol. Palaeoecol.* **137**, 55-77

CLIMAP Project Members (1976) The surface of the ice-age earth. *Science* **191,** 1131-1137.

Cronblad H.G. and Malmgren B.A. (1981) Climatically controlled variation of Sr and Mg in Quaternary planktic foraminifera. *Nature* **291,** 61-64.

Deuser W.G. (1978) Stable-sotope paleoclimatology: a possible measure of past seasonal contrast from foraminiferal tests. *N. Z. Dep. Sci. Ind. Res. Bull.* **220,** 55-60.

Deuser W.G., Ross E.H., Hemleben C., and Spindler M. (1981) Seasonal changes in species composition, numbers, mass, size, and isotopic composition of planktonic foraminifera settling into the deep Sargasso Sea. *Palaeogeogr.,Palaeoclimatol., Palaeoecol.* **33,** 103-127.

Epstein S., Buchbaum R., Lowenstam H., and Urey H.C. (1951) Carbonate-water isotopic temperature scale. *Geol. Soc. America Bull.* **62,** 417-426.

Emiliani C. (1954) Depth habitats of some species of pelagic foraminifera as indicated by oxygen isotope ratios: *Am. Jour. Sci.*. **252,** 149-158.

Emiliani C. (1955) Pleistocene Temperatures. *Jour. Geology* **63,** 538-578.

Emiliani C. (1966) Paleotemperature analysis of Caribbean cores P6304-8 and P6304-9 and a generalized temperature curve for the past 425,000 years. *Jour. Geology* **74,** 109-126.

Erez J., and Luz B. (1983) Experimental paleotemperature equation for planktonic foraminifera. *Geochim. Cocmochim. Acta* **47,** 1025-1031.

Erez J., Almogi-Labin A., and Avraham S. (1991) On the life history of planktonic foraminifera: lunar reproduction cycle in *Globigerinoides* sacculifer (Brady). *Paleoceanography* **6,** 295-306.

Fairbanks R.G., Sverdlove M., Free R., Wiebe P.H., and Be A.W.H. (1982) Vertical distribution and isotopic fractionation of living planktonic foraminifera from the Panama Basin. *Nature* **298,** 841-844.

Fairbanks R.G., Wiebe P.H., and Be A.W.H. (1980) Vertical distribution and isotopic composition of living planktonic foraminifera in the Western North Atlantic. *Science* **207,** 61-63.

Fairbanks R.G. and Wiebe P.H (1980) Foraminifera and chlorophyll maximum: vertical distribution, seasonal succession, and paleoceanographic significance. *Science* **209,** 1524-1526.

Faul K.L., Ravelo C.A., and Delaney M.L. (2000) Reconstructions of upwelling, productivity, and photic zone depth in the Eastern Equatorial Pacific Ocean using planktonic foraminiferal stable isotopes and abundances. *J. Foraminiferal Res.* **30,** 110-125.

Fenton M., Geiselhart S., Rohling E.J. Hemleben C. (2000) Aplanktonic zones in the Red Sea. *Mar. Micropalenontology* **40,** 277-294.

Hamilton P. (1992) Lower continental slope cyclonic eddies in the Central Gulf of Mexico. *J. of Geophys. Res.* ***97*****,** 2185-2200.

Hemleben C., Spindler M., and Anderson O.R. (1989) *Modern Planktonic Forminifera.* Springer Velag.

Hillaire-Marcel C., de Vernal A., Bilodeau G., And Weaver A.J. (2001) Absence of deep –water formation in the Labrador Sea during the last interglacial period. *Nature* **410,** 1073-1077.

Kohfeld K.E., Anderson R.F., and Lynch-Stieglitz J. (2000) Carbon isotpic disequilibrium in polar planktonic foraminifera and its impact on modern and Last Glacial Maximum reconstructions. *Paleoceanography* **15,** 53-64.

Lea D.W., Mashiotta T.A., and Spero H.J. (1999) Controls on magnesium and strontium uptake in planktonic foramininifera determined by live culturing. *Geochim. Cocmochim. Acta* **63,** 2669-2379.

Lea D.W., Pak D.K., and Spero H.J. (2000) Climate impact of late Quaternary Equatorial Pacific sea surface temperature variations. *Science* **289,** 1719-1724.

Leipper D.F. (1970) A sequence of current patterns in the Gulf of Mexico. *J. of Geophys. Res. 7***5,** 637-657.

Lin L., Peterson L.C., Overpeck J.T., Trumbore S.E. and Murray D.W. (1997) Late Quaternary climate change from $\delta^{18}O$ records of multiple species of planktonic foraminifera: High-resolution records from the anoxic Cariaco Basin, Venezuela. *Paleoceanography* **12,** 415-427.

Mortyn P.G., Charles C.D., Hodell D.A. (2002) Southern Ocean upper water column structure over the last 140 kyr with emphasis on the glacial terminations. *Global Planet. Change* **34,** 241-252.

Nürnberg D., Bijma J. and Hemleben C. (1996a) Assessing the reliability of magnesium in foraminiferal calcite as a proxy for water mass temperatures. *Geochim. Cosmochim. Acta* **60,** 803-814.

Nürnberg D., Bijma J. and Hemleben C. (1996b) Erratum assessing the reliability of magnesium in foraminiferal calcite as a proxy for water mass temperatures. *Geochim. Cosmochim. Acta* **60,** 2483-2384.

Oberhänsli H., Bénier C., Meinecke G., Schmidt H., Schneider R., and Wefer G. (1992) Planktonic foraminifers as tracers of ocean currents in the Eastern South Atlantic. *Paleoceanography* **7,** 607-632.

Ortiz J.D., Mix A.C., and Collier R.W. (1995) Environmental control of living symbiotic and asymbiotic foraminifera of the California current. *Paleoceanography* **10,** 987-1009.

Ottens J. (1991) Planktic foraminifera as North Atlantic water mass indicators. *Oceanologica Acta* **14,** 123-140.

Parker F.L. (1962) Planktonic foraminiferal species in Pacific sediments. Micropaleontology **8,** 219-254.

Peeters F.J.C., Brummer G.A., Ganssen G. (2002) The effect of upwelling on the distribution and stable isotope composition of *Globigerina bulloides* and *Globigerinoides ruber* (planktic foraminifera) in modern surface waters of the NW Arabian Sea. *Global Planet. Change* **34,** 269-291.

Peterson L.C., Overpeck J.T., Kipp N.G., and Imbrie J. (1991) A high-resolution late Quaternary upwelling record from the anoxic Cariaco Basin, Venezuela. *Paleoceanography* **6,** 99-119.

Reiss Z., Halicz E., and Luz B. (1999) Late-Holocene foraminifera from the SE Levantine Basin. *Israel Journal of Earth Sciences.* **48,** 1-27.

Rosenthal Y., Lohmann G.P., Lohmann K.C., and Sherrell R.M. (2000) Incorporation and preservation of Mg in *Globigerinoides sacculifer*: Implications for reconstructing the temperature and $^{18}O/^{16}O$ seawater. *Paleoceanography* **15**, 135-145.

Savin S.M. and Douglas R.G. (1973) Stable isotope and magnesium geochemistry of recent planktonic foraminifera from south Pacific. *Geol. Soc. Am. Bull.* **84,** 2327-2342.

Schiebel R., Bijma J., and Hemleben C. (1997) Population dynamics of the planktic foraminifer *Globigerina bulloides* from the eastern North Atlantic. *Deep-Sea Res.* **44**, 1701-1713.

Schiebel R., Waniek J., Bork M., and Hemleben C. (2001) Planktic foraminiferal production stimulated by chlorophyll redistribution and entrainment of nutrients. *Deep-Sea Res.* **48,** 721-740.

Schmuker B., Hilbrecht H., and Schielbel R. (2000) Modern planktic foraminifera in the Eastern Carribean Sea and their relation with the physico-chemical environment. Ocean Sciences Meeting. San Antonio, Texas. OS 42A-13 Poster.

Shackleton N.J., and Opdyke N.D. (1973) Oxygen isotope and paleomagnetic stratigraphy of equatorial Pacific core V228-238: oxygen isotope temperature and ice volumes on a 10^5 year and 10^6 year scale. *Quat. Res.* **3,** 39-55.

Spero H.J. (1998) Life history and stable isotope geochemistry of planktonic foraminifera. In *Isotope Paleobiology and paleoecology* (eds. R. Norris and R.M. Corfield), pp 7-36. The Paleontological Society.

Synder S. (1978) Distribution of planktonic foraminifera in surface sediments of the Gulf of Mexico. *Tulane studies in Geology and Paleontology.* **14,** 1- 80.

Takahashi K., and Bé A.W.H. (1984) Planktonic foraminifera: factors controlling sinking speeds. *Deep Sea Res.* **31,** 1477-1500.

Thunell R.C. and Honjo S. (1981) Calcite dissolution and the modification of planktonic foraminiferal assemblages. *Mar. Micropaleo.* **6,** 169-182.

Ufkes E., Jansen J.H.F., Brummer G.A. (1998) Living planktonic foraminifera in the eastern South Atlantic during spring: indicators of water masses, upwelling and the Congo (Zaire) River plume. *Mar. Micropaleo.* **33,** 27-53.

Vance D., and Burton K. (1999) Neodymium isotopes in planktonic foraminifera: a record of the response of continental weathering and ocean circulation rates to climate change. *Earth Planet. Sci. Lett.* **173,** 375-379.

Watkins J.M., Mix A.C., and Wilson J. (1996). Living foraminifera: tracers of circulation and productivity regimes in the central Pacific. *Deep Sea Research II.* **43.** 1257-1282.

Wiebe P.H., Burt K.H., Boyd S.H, and Morton A.W. (1976) A multiple opening /closing net environmental sensing system for sampling zooplankton. *J. Mar Res.* **34**, 313-326.

Williams D.F., Bé A.W.H., Fairbanks R.G. (1979). Seasonal oxygen isotopic variations in living planktonic foraminifera off Bermuda. *Science* **206,** 447-449.

Williams D.F., Sommer M.A. II, and Bender M.L. (1977) Carbon isotopic compositions of recent planktonic foraminifera of the Indian Ocean. *Ear. Plan. Sci. Let.* **36,** 391-403.

Wiseman W. J., and Sturges W. (1999) Physical oceanography of the Gulf of Mexico: Processes that Regulate its Biology. In: *The Gulf of Mexico Large Marine Ecosystem Assesment, Sustainability, and Management* (ed. H. Kumpf et al.), pp. 77-92. Backwell Science.

Wormuth J.H. (1981) Vertical distributions and diel migrations of Euthecosomata in the northwest Sargasso Sea. *Deep-Sea Res.* **28A**, 1493-1515.

Wormuth J.H., Ressler P.H., Cady R.B., and Harris E.J. (2000a) Chapter 3 Biological Oceanography. In *Cetaceans, sea turtles and seabirds in the northern Gulf of Mexico: distribution, abundance and habitat associations.* Vol. II: Technical report (eds Davis R.W., Evans W.E., and Würsig B.)

Wormuth J.H., Ressler P.H., Cady R.B., and Harris E.J. (2000b) Zooplankton and Micronekton in cyclones and anticyclones in the Northeast Gulf of Mexico. *Gulf of Mexico Science.* 23-34.

Zimmerman and Biggs D.C. (1999) Patterns of distribution of sound-scattering zooplankton in warm- and cold-core eddies in the Gulf of Mexico, from an arrowband acoustic Doppler current profiler survey. *J. of Geophys. Res.* **104**, 5251-5262.

APPENDIX A (MATLAB scripts of interest)

```
%Below script works to convert MOC column data to variable width bar
%graph data
%SOME STATEMENTS POSSIBLY WRAPPED AROUND to next line in transfer - %
      will cause bugs
%  ESPECIALLY SOME COMMENTS.that need initial '%' character

%Script modified from previous version "data_interval_script2" to
%     create depth, temp, and density gradient arrays for each tow
%DOES ONE TOW AT A TIME
%Load Hydrographic_edge_values&abundances_num_m-2   %Holds edge net %
      values (depth,temp,sigma);
%     variable are in first three columns and then
%     species abundances (#m-2)start in column 6 in the order given
%     in 'gtitle' in next program

%uses values from CTD#7 and revised files
%does not have missing nets as G_MOC#m-3 does

%Load I_MOC#m-2d                                        %Holds average net
%values (depth,temp,sigma)
                                                        % ARE THESE NEEDED?
%?x & y values are from I_MOC#m-2c data
%?x2 & y2 are being determined

clear x2 y2 x y nets
net_number=8;

t=1                                          %MUST CHANGE FOR EACH TOW
%for t=1:4;
%use 'nets' for G_MOC's/tow and 'net_number' for MOC's/avg_tow
if     t==1; tow=G_MOC208;                                      %
avg_tow=MOC208;
elseif t==2; G_MOC209(1,1)=0; tow=G_MOC209; net_number=9;   %
avg_tow=MOC209;
elseif t==3; G_MOC217(1,1)=0; tow=G_MOC217; net_number=9;   %
avg_tow=MOC217
elseif t==4; G_MOC218(1,1)=0; tow=G_MOC218;             ;   %
avg_tow=MOC218;
end

nets=1:net_number;
%Range Script - Creates Depth, Temperature, and Sigma Interval values
%     from Edge values
%               Creates Edge x & y values
%               Some values don't necessarily change monotonically,
%     so use abs


for d_arrays=1:3;                                  %d_arrays refers
%     to each data column: depth, temp, sigma
    x(nets,d_arrays)=abs((tow(nets+1,d_arrays)-
tow(nets,d_arrays)));%Intervals of depth,temp,sigma per net
    if d_arrays==1
        multi=-10;              %spacers need to increase w/ depth
```

```
  %      y=tow(nets,species);    %DO NOT divide by property for depth
    elseif d_arrays==2;
        %x(nets,d_arrays)=-x(nets,d_arrays);
        multi=1;               %temp data decrease w/ depth, so spacing
    else
        multi=-.3;                  %spacers need to increase w/ depth
    end %if_d_arrays
%%%%%%%%%%%%%%%%%%%%%%%%%%%%
for species=6:14;
    %%if d_arrays==1                %Loop to not divide depth data
    %%     y=tow(nets,species);
    %      hello='not dividing concnetrations'
    %%else
            y=tow(nets,species)./x(nets,d_arrays);       %
    %       hello='dividing concentrations'
    %%end %end if d_arrays
%%End Range script%

%%%%%%%%%%%%%%%%%%%%%%%%%%%%
%Spacer script & repeat X w/ zero Y's with data in one column format
%Script below takes data from column and repeats row values for
variable width
%Change 'spacer' below & 'multi' above for gap wanted
spacer=.05;base=0;
    for j=1:5*net_number;
          if rem(j,5)==0                        %index 5,10,15,20,25 -
%     creates gap
              x2(j,d_arrays)=tow((j/5)+1,d_arrays)-multi*spacer;
              y2(j,species,d_arrays)=base;
          elseif rem((j+1),5)==0                %index 4,9,14,19,24 -
%     last pt of bar
              x2(j,d_arrays)=tow((j+1)/5+1,d_arrays);
              y2(j,species,d_arrays)=base;
          elseif rem((j+2),5)==0                %index 3,8,13,18,23 -
%     top lft corner bar
              x2(j,d_arrays)=tow((j+2)/5+1,d_arrays);
              y2(j,species,d_arrays)=y((j+2)/5);
          elseif rem((j+3),5)==0                %index 2,7,12,17,22,27
%     - top rt corner bar
              x2(j,d_arrays)=tow((j+3)/5,d_arrays)-multi*2*spacer;
              y2(j,species,d_arrays)=y((j+3)/5);
          elseif rem((j+4),5)==0                %index 1,6,11,16,21,26
%     - start of bar
              x2(j,d_arrays)=tow((j+4)/5,d_arrays)-multi*2*spacer;
              y2(j,species,d_arrays)=base;
          end                                   %Ends if
      end                                       %Ends for j
end                                             %Ends for species
end                                             %Ends for d_arrays

%end                                             %t
%%%%%%%%%%%%%%%%%%%%%%%%%%%%
%save as appropriate tow data
%save x2_y2_MOCs_data_interval_script_abs_Output5
```

```
% ...x2_MOC217 y2_MOC217
%contains new data in
%  MOC209 NET1 & new density numbers from CTD7 for MOC217&MOC218

h=area(x2(:,d_arrays),y2(:,6,d_arrays))
%rotate(h,[0 0 1],-90,[0 0 0])                    %See Help to see axis
of rotation Z-axis
%axis([0 50 -31 -13])                            %Transforms co-ords
%set(gca,'Ydir','reverse', 'YTickLabel',[30 28 26 24 22 20 18 16
14])%fix co-ords from rotate

 %   xlabel('Individuals m^{-3}{\circ}C^{-1}','FontSize', 14);
               %  ylabel('Temperature {\circ}C','FontSize',14);
```

```
%Var width barh each species all tows (4X3) #/m2 per STD vs Nets
%(Depth), Temperature, & Sigma
%Use data created in 'data_interval_script5' & and manually saved into
%'x2_MOC's & y2_MOC's'
%% divides by range found in net e.g. #m-2 / by depth range not by
%average

% load 'x2_y2_MOCs_data_interval_script_abs_Output5' for plot data -
%   contains depth data as m-3, remaining data as in ..._Output.mat;

% load 'Hydrographic_MOC_data_revised';
%contains salinity, temperature, density, depth, density anomaly data


fig_start=12;                                %Figure numbers start after
plotrow=4;plotcolumn=3;                           %subplot array
font='TimesNewRoman';%'MyriadRoman';
%% Graph extents in subplot scripts below
int_text=[-175 -175 -175 -150 -110 -100 -80 -70 -175];
% Int. Values height placement in graphs
FSize=10;Titles_FZize=14;                      %Label text size

gtitle=char('O. universa','G. ruber, var. pink',...
             'G. ruber, var. white',...
            'G. sacculifer','H. pelagica','G. bulloides',...
            'G. siphonifera','G. calida','G. menardii')

clf
for j=3:9;%1:9;                 %'j' refers to 'gtitle' species names

figure(j);                            %Creates Figure for each species
                                          %#1-9
p_index=1;                            %subplot index
species=j+5;                          %'species' refers to columns in
%                                         data w/species abund

%       DATA ARRAY ACCESS %%%%%%%%%%%%%%%%%%%%%%%%%%%%%%%%%%%%%%%%%%%%%%%%
for t=1:4;
    if t==1                       % MOC 208
sp_int = [7.52 3.15 0.17 1.75 4.47 0.33 6.09 3.88 8.00];%%MOCNESS 208
Species integrated values
x2=x2_MOC208; y2=y2_MOC208; title_text='MOCNESS 208'; % - Antiyclonic';
temp=Hydro_MOC208(:,2); depth=Hydro_MOC208(:,4);

    elseif t==2                   % MOC 209
sp_int = [4.96 0.36 0.00 0.80 1.00 0.00 2.80 3.68 9.91];%MOCNESS 209
Species integrated values
x2=x2_MOC209;y2=y2_MOC209; title_text='MOCNESS 209';% - Anticyclonic';
temp=Hydro_MOC209(:,2); depth=Hydro_MOC209(:,4);

    elseif t==3                   % MOC217
sp_int = [4.57 13.06 0.85 7.34 2.39 21.53 1.81 4.53 5.35];%MOC 217
Species integrated values
```

```
x2=x2_MOC217;y2=y2_MOC217; title_text='MOCNESS 217';% - Cyclonic';
%
temp=Hydro_MOC217(:,2); depth=Hydro_MOC217(:,4);

    elseif t==4;                    % MOC218
sp_int = [5.42 26.41 1.44 26.43 4.26 34.87 22.84 1.45 7.16];%MOC 218
Species integrated values
x2=x2_MOC218;y2=y2_MOC218; title_text='MOCNESS 218';% - Cyclonic';
%
temp=Hydro_MOC218(:,2); depth=Hydro_MOC218(:,4);

end                                             % End of if t
%                       %%%%%%%%%%%%%%%%%%%%%%%%%%%%%%%%%%%%%%%%%%%%%%%%

%                                       PLOT ROUTINES
%Loop does 208 properties, then does 209, etc.
%                       %%%%%%%%%%%%%%%%%%%%%%%%%%%%%%%%%%%%%%%%%%%%%%%%
%                       %%%%%%%%%%%%%%%%%%%%%%%%%%%%%%%%%%%%%%%%%%%%%%%%
%                                       DEPTH - d_arrays=1
subplot(plotrow,plotcolumn,p_index);

if max(y2(:,species,1))==0
    plot(xlimits,zeros(size(xlimits)))
else
    area(y2(:,species,1),x2(:,1),'EdgeColor','White');
end

xMax=get(gca,'XLim');
yMax=get(gca,'YLim');

%                       %%%%%%%%%%%%%%%%%%%%%%%%%%%%%%%%%%%%%%%%%%%%%%%%
%                       Set various depth, temp, & sigma  x-axis limits
if species==8
    xlimits=[0 75];txlimits=20*xlimits;sxlimits=20*xlimits; %
elseif  species==13
    xlimits =[0 150];txlimits=[0 6000];sxlimits=[0 6000]; ;
    %elseif t==3 &(species==7 | species==11)         %Also set x-axis
extents
    %xlimits= [0 400];
elseif (t==4 | t==3) &(species==7 | species==9)
    xlimits = [0 900];txlimits=[0 6000];sxlimits=[0
6000];%txlimits=xlimits;sxlimits=xlimits;
elseif (t==4 | t==3) &(species==11)
    xlimits = [0 900];txlimits=[0 6000];sxlimits=[0 12000]
else xlimits =[0 150];txlimits=[0 6000];sxlimits=[0 6000]; ;
end                                             %

%mauel override of script limit making below
%txlimits=[0 300];sxlimits=[0 300];
axis([xlimits 0 225]); %Use this if not using double's values
%axis auto
%                       %%%%%%%%%%%%%%%%%%%%%%%%%%%%%%%%%%%%%%%%%%%%%%%%
%                                  set axis properties
ylabel(title_text,'Fontsize',10,'FontWeight','demi','FontName',font);
```

```
%Subplot titles
%ylabel('Individuals m^{-2}','FontSize', FSize);-PUT THESE BACK IN
ILLUSTRATOR

%'XTickLabel',[],...
%    'FontName',font,...
%    'YTickLabel',[200:-50:0]);%Warning1='Y-axis values are assigned'
%fix co-ords from rotate)
if (p_index==1 | p_index==10)
    xlabel('Individuals m^{-3}','FontSize',FSize,'FontName',font)
 %   set(gca,'XTickLabelMode','auto')
end
if(p_index==1)
    set(gca,'XAxisLocation','top');% Xlabels on top
end;

%                                          Integrated Value
text(xMax(2)*.25,-int_text(j),['{\Sigma} =
',num2str(sp_int(j),'%2.2f'),' #m^{-2}'],'Color','red')

%                                             Species Caption
if p_index==10
    str1=['  Figure ',num2str(j+fig_start),'.  \rm',...
          '\it',gtitle(j,:)];
%,'\rm depth profiles: concentration m^{-3}, temperature (m^{-
%3}{\circ}C^{-1}), '];
    str2=['density ','(m^{-2}{\sigma}^{-1}).  Respective integrated tow
abundances given in red.  ',...
         '                                    '];

text(.25*xMax(1),yMax(2)/2,[str1],'FontAngle','normal','FontSize',...
Titles_FZize)
end%end if of Species Caption placement

%*****************************  Script below from double-text
basically from Help menu  *******
ax1 = gca;
set(ax1,'XColor','k','YColor','k')

ax2 = axes('Position',get(ax1,'Position'),...
           'XAxisLocation','top',...
           'YAxisLocation','right',...
           'Color','none',...
           'XColor','r','YColor','r');

hl2 = line(temp,depth,'Linestyle','-','Color','r','Parent',ax2);

%xlimits = [0 150];%get(ax1,'XLim'); USE ABOVE LOOP VALUES TO SET %
                                     'xlimits';
xlimits2 = [14 32];%get(ax1,'XLim');
ylimits = [0 225];%get(ax1,'YLim');
set(ax1,'XLim',xlimits,'YLim',ylimits);
set(ax2,'XLim',xlimits2,'YLim',ylimits)
```

```
%xinc1 = 50;
xinc1 = (xlimits(2)-xlimits(1))/3;
xinc2 = (xlimits2(2)-xlimits2(1))/3;%3%three will line up with other %
                                                    original axis ticks;
yinc = 50;%(ylimits(2)-ylimits(1))/4;
%Now set the tick mark locations.

set(ax1,'Ydir','reverse','XTick',[xlimits(1):xinc1:xlimits(2)],...
        'YTick',[ylimits(1):yinc:ylimits(2)])


set(ax2,'YDir','reverse','XTick',[],...%[xlimits2(1):xinc2:xlimits2(2)]
,...
        'YTick',[]);%[ylimits(1):yinc:ylimits(2)])


%axis auto

%*****************************  Script above from double-text
basically from Help menu  *******

%                        %%%%%%%%%%%%%%%%%%%%%%%%%%%%%%%%%%%%%%%%%%%%%%%%
%                        %%%%%%%%%%%%%%%%%%%%%%%%%%%%%%%%%%%%%%%%%%%%%%%%
%                                TEMPERATURE - d_arrays=2
subplot(plotrow,plotcolumn,p_index+1);
if max(y2(:,species,2))==0
    plot(txlimits,zeros(size(txlimits)))
else
    area(y2(:,species,2),x2(:,2),'EdgeColor','White');
end

xMax=get(gca,'YLim');
yMax=-get(gca,'XLim');

%axis auto
%axis([0 1000 13 31])
axis([txlimits 13 31])
%axis([0 8 13 31])

%ylabel('Temperature ({\circ}C)','FontSize', FSize,'FontName',font)

%set(gca,'color','none',...
%set(gca,'Ydir','reverse')
%,...
 %       'FontName',font,...
  %      'XTickLabel',[],...
  %     'YTickLabel',[30:-5:15]);Warning2='Y-axis values are assigned'
%fix co-ords from rotate)

txinc1 = (txlimits(2)-xlimits(1))/3;
if(p_index+1==2)                                % Xlabels on top

set(gca,'XAxisLocation','top','XTick',[txlimits(1):txinc1:txlimits(2)])
     xlabel('Individuals m^{-2}{\circ}C^{-1}',...
```

```
'FontSize',FSize,'FontName',font)
elseif( p_index+1==11)                                  % Xlabels on bt
    set(gca,'XAxisLocation','bottom','XTick',[sxlimits(1):...
sxinc1:sxlimits(2)])
     xlabel('Individuals m^{-2}{\circ}C^{-1}',...
'FontSize',FSize,'FontName',font)
else
    set(gca,'XTick',[txlimits(1):txinc1:txlimits(2)],'XTickLabel',[]);
end;

%                       %%%%%%%%%%%%%%%%%%%%%%%%%%%%%%%%%%%%%%%%%%%%%%%%
%                       %%%%%%%%%%%%%%%%%%%%%%%%%%%%%%%%%%%%%%%%%%%%%%%%
                                                %Sigma
subplot(plotrow,plotcolumn,p_index+2);

if max(y2(:,species,3))==0
    plot(sxlimits,zeros(size(sxlimits)))
else
    area(y2(:,species,3),x2(:,3),'EdgeColor','White');
end

xMax=get(gca,'YLim');
yMax=get(gca,'XLim');

%axis auto
axis([sxlimits 20 27]);                %Set all axis scales the same
%axis([0 8 20 27]);

%ylabel('Density ({\sigma})','FontSize', FSize,'FontName',font)
sxinc1 = (sxlimits(2)-sxlimits(1))/3;
if(p_index+2==3)                                % Xlabels on top

set(gca,'XAxisLocation','top','YDir','reverse','XTick',[sxlimits(1):sxi
nc1:sxlimits(2)])
    xlabel('Individuals m^{-2}{\sigma}^{-1}',...
'FontSize',FSize,'FontName',font)
elseif( p_index+2==12)                                  % Xlabels on bt

set(gca,'XAxisLocation','bottom','YDir','reverse','XTick',[sxlimits(1):
sxinc1:sxlimits(2)])
    xlabel('Individuals m^{-2}{\sigma}^{-1}',...
'FontSize',FSize,'FontName',font)
else

set(gca,'XTick',[sxlimits(1):sxinc1:sxlimits(2)],'YDir','reverse','XTic
kLabel',[]);
end;

p_index=p_index+plotcolumn;

%if t==2 text(xMax(2)*.5,-yMax(2)*1.17,...
['Figure ',num2str(j+fig_start)],...
 %       'FontWeight','demi','FontSize',Titles_FZize);%Figure Number
 %end%end if of Main title placement
```

```
end                                                % End of t determining
tow & properties

%    Print parameters    %%%%%%%%%%%%%%%%%%%%%%%%%%%%%%%%%%%%%%%%%%%%%%%%
width=5.95;height= 7.25;leftmargin=1.4;bottommargin=2.5;

set(gca,'FontName',font)
set(gcf,'PaperOrientation','portrait',...
    'PaperPosition',[leftmargin, bottommargin,width, height],...
    'PaperSize',([width, height]),'PaperType','usletter')
%    'PaperSize',([width+.5, height+.5]),'PaperType','usletter')
%   PaperOrientation = 'landscape'
%width=8.5;height=5.95;leftmargin=1.25;bottommargin=1.4;
%     PaperPositionMode = manual
% set driver to black & white printer -
% search print & command line in help navigator
%Graphics: Basic Printing and Exporting: Changing the Figure's Settings

end %Ends for j
```

VITA

Sharath Reddy Ravula was born on October 21, 1970 in Algiers, Algeria as a citizen of India. His interest in oceanography probably stems from experiences in North Africa and Southern Europe during his first seven years. He considers himself a Texan, however, since he spent the majority of his life in Alief, Texas, a suburb of Houston. Afterwards, he attended Columbia University in New York City for four years where he graduated with a degree in mechanical engineering in May of 1992. For a year and a half before beginning his graduate career, he worked as an engineer in a fabrication shop designing Constant Spring Hangers, Pipe Supports, and Pressure Vessels. He lost his first advisor after four years in Aggieland, but decided to continue with another advisor, the smashingly handsome and witty Niall Slowey. Incredibly, he has been financially supported from when he started in the Fall of 1995. He also was sent across the Gulf of Mexico to Key West, FL for a week; to Woods Hole, MA for six weeks; along the Hawaiian Islands for three weeks; and to Southeast Atlantic along the South African and Namibian coast for over two months. He would be happy to answer questions or comments. He can be reached through his address or email below:

1105 Buttercup Circle
College Station, TX 77845
sharath@ocean.tamu.edu